

# Generalized Matrix Decomposition Regression: Estimation and Inference for Two-way Structured Data

Yue Wang, Ali Shojaie, Timothy W. Randolph and Jing Ma

October 11, 2021

## Abstract

This paper studies high-dimensional regression with two-way structured data. To estimate the high-dimensional coefficient vector, we propose the generalized matrix decomposition regression (GMDR) to efficiently leverage any auxiliary information on row and column structures. The GMDR extends the principal component regression (PCR) to two-way structured data, but unlike PCR, the GMDR selects the components that are most predictive of the outcome, leading to more accurate prediction. For inference on regression coefficients of individual variables, we propose the generalized matrix decomposition inference (GMDI), a general high-dimensional inferential framework for a large family of estimators that include the proposed GMDR estimator. GMDI provides more flexibility for modeling relevant auxiliary row and column structures. As a result, GMDI does not require the true regression coefficients to be sparse; it also allows dependent and heteroscedastic observations. We study the theoretical properties of GMDI in terms of both the type-I error rate and power and demonstrate the effectiveness of GMDR and GMDI on simulation studies and an application to human microbiome data.

*Keywords:* Dimension reduction; high-dimensional inference; prediction; two-way structured data

# 1 Introduction

High-dimensional data with structures among the variables (columns) and samples (rows), termed two-way structured data hereafter, are becoming increasingly common in ecology, biology, and neuroscience. Informative two-way structures can often be obtained from various auxiliary sources a priori. In many applications, the goal is to examine associations between such structured data and an outcome of interest. The application that motivated this research comes from human microbiome studies, where it is important to study how bacterial genetic variations affect host health. However, unlike studies in human genomics where it is important to account for within-family correlation, human microbiome composition may be more dependent on environment, diet, and culture than host genetics (Zeevi et al., 2019). Therefore, it may be more relevant to account for metagenomic similarities between samples in these analyses. Also, microbes are closely related via the phylogenetic tree, a branching diagram that shows the evolutionary relationship between microbes. This motivates our development of a high-dimensional linear regression framework to examine associations between a large number of covariates and an outcome of interest, while efficiently leveraging auxiliary row and column structures, such as metagenomic similarities between samples and phylogenetic similarities between microbes.

## 1.1 High-dimensional Inference with Two-way Structured Data

In this paper, we consider the following linear model

$$\mathbf{y} = \mathbf{X}\boldsymbol{\beta}^* + \boldsymbol{\epsilon}, \tag{1}$$

where  $\mathbf{X} \in \mathbb{R}^{n \times p}$  denotes a data matrix with potential row and column structures,  $\mathbf{y} \in \mathbb{R}^n$  is the outcome of interest, and  $\boldsymbol{\beta}^* \in \mathbb{R}^p$  is the underlying true regression coefficient. We allow  $p$  to be greater than  $n$ . In addition, we assume that  $\boldsymbol{\epsilon}$  is a vector of random noises such that  $\mathbb{E}[\boldsymbol{\epsilon} \mid \mathbf{X}] = \mathbf{0}_n$  and  $\text{Cov}(\boldsymbol{\epsilon} \mid \mathbf{X}) = \boldsymbol{\Psi}$ , where  $\mathbf{0}_n$  is an  $n \times 1$  vector of zeros, and

$\Psi$  is an  $n \times n$  covariance matrix. We do *not* assume that entries of  $\epsilon$  are *i.i.d.*, as the samples may be correlated and heteroskedastic, as captured by  $\Psi$ . Let  $\mathbf{H} \in \mathbb{R}^{n \times n}$  and  $\mathbf{Q} \in \mathbb{R}^{p \times p}$  denote two auxiliary positive definite matrices. We assume that entries of  $\mathbf{H}$  and  $\mathbf{Q}$ , respectively, inform similarity between samples and between variables with the effect of other samples and variables removed, termed *conditional* similarity hereafter. The  $\Psi$  and  $\mathbf{H}$  are related, and their connection will be discussed in Section 3.1. We assume that  $\mathbf{X}$ ,  $\mathbf{H}$  and  $\mathbf{Q}$  are deterministic quantities, and refer to the triple  $(\mathbf{X}, \mathbf{H}, \mathbf{Q})$  as two-way structured data hereafter. Throughout the article, we assume that  $\mathbf{X}$  and  $\mathbf{y}$  are appropriately centered such that  $\mathbf{1}_n^\top \mathbf{H} \mathbf{y} = 0$  and  $\mathbf{1}_n^\top \mathbf{H} \mathbf{X} = \mathbf{0}_p^\top$ , where  $\mathbf{1}_n$  is an  $n \times 1$  vector of all ones. We will study estimation and inference of the high-dimensional parameters  $\beta^*$ , while leveraging information from  $\mathbf{H}$  and  $\mathbf{Q}$ .

Most existing high-dimensional inference (HDI) tools assume that samples are *i.i.d.*, which may not hold if complex row structures exist. Ignoring such row structures may lead to incorrect inference even in low-dimensional settings. Furthermore, existing HDI tools, including Bühlmann (2013); Zhang and Zhang (2014); van de Geer et al. (2014); Zhao and Shojaie (2016); Ning and Liu (2017); Zhu and Bradic (2018), all require at least one of the following assumptions: (i)  $\beta^*$  is sparse, (ii)  $\mathbf{X}$  satisfies a restricted eigenvalue-type condition if a fixed design is considered, and (iii) the precision matrix of the variables in  $\mathbf{X}$  has row sparsity if a random design is considered. However, these conditions may fail when strong correlations exist among the variables, which is common for two-way structured data. Indeed, we provide an example in Section 5 where all three assumptions are probably violated. Specifically, in this example, most covariates are marginally associated with the outcome (see Fig. 5 for details). Two possible explanations for the large number of marginal associations may be that (i) a large number of the covariates are also conditionally associated with the outcome; (ii) these covariates are highly correlated, but only a few of these are conditionally associated with the outcome. In the first situation, the vector of regression coefficients is not sparse; in the second situation, any restricted eigenvalue-type condition may fail (see van de Geer et al. (2009) for more discussions), and likely, the

precision matrix of the covariates is not sparse.

## 1.2 Our Contribution

This paper introduces the generalized matrix decomposition regression (GMDR), a dimension-reduction based estimation procedure that efficiently leverages any pre-specified two-way structures. The GMDR is built upon the generalized matrix decomposition (GMD, Allen et al. (2014); Escoufier (2006)), which extends the singular value decomposition (SVD) to incorporate auxiliary two-way structures. Thus, GMDR can be viewed as an extension of the principal component regression (PCR) for analyzing two-way structured data. However, unlike PCR which uses top principal components as the predictors, our GMDR selects the GMD components that are most predictive of the outcome. This novel selection procedure ensures more accurate prediction using GMDR.

We then define a broad class of estimators for high-dimensional regression on two-way structured data that includes the proposed GMDR and many classical methods, such as the principal component regression and ridge regression. We develop the GMD inference (GMDI) framework, an HDI procedure that can assess the significance of individual variables based on any arbitrary estimator in this class. The GMDI assumes that the pre-specified row and column structures can, respectively, inform the covariance among the samples and the structure of the regression coefficients. As a result, GMDI does not require the true regression coefficients to be sparse, allows dependent and heteroscedastic samples, and provides more flexibility for users to specify relevant auxiliary row and column structures.

The GMDI follows the general idea of bias correction for ridge-type estimators but uses a novel initial estimator that efficiently leverages the pre-specified two-way structures. We derive the asymptotic distribution of the bias-corrected estimator. Based on this, we construct asymptotically valid two-sided p-values and provide sufficient conditions under which GMDI offers guaranteed power. Our numerical studies demonstrate the superior per-

formance of GMDI for two-way structured regression compared to existing HDI methods, even when pre-specified structures are not fully informative.

### 1.3 Related Literature

Methods for incorporating auxiliary information into high-dimensional linear regression have received much recent interest. For example, network-constrained regularization approaches have been developed to incorporate prior knowledge on the structures of the variables (Li and Li, 2008, 2010). The more recent kernel penalized regression (KPR, Randolph et al. (2018)) can incorporate pre-specified two-way structures using a generalized least squares formulation with a kernel-guided  $l_2$  type penalty. However, there is a paucity of methods that can provide inference for associations between an outcome and the high-dimensional two-way structured covariates. This paper bridges this gap by developing an effective HDI procedure for a broad class of estimators that encompasses the existing KPR.

### 1.4 Organization and Notation

The rest of the article is organized as follows. In Section 2, we first introduce the GMDR estimation/prediction framework, accompanied by the novel selection procedure of the GMD components. We then link the GMDR estimator to a broad class of estimators. In Section 3, we present the GMDI procedure for any arbitrary estimator in this class and explain the rationale behind the key assumptions for GMDI. Multiple simulation studies that examine the finite-sample performance of GMDI are presented in Section 4. In Section 5, we demonstrate the effectiveness of GMDR and GMDI on an application to microbiome data. Section 6 summarizes our findings and outlines potential extensions. Technical proofs are provided in the Appendix.

Throughout the paper, we use normal typeface to denote scalars, bold lowercase typeface to denote vectors and bold uppercase typeface to denote matrices. For any vector  $\mathbf{v} \in \mathbb{R}^p$ ,

we use  $v_j$  to denote the  $j$ -th element of  $\mathbf{v}$  for  $j = 1, \dots, p$ . For any matrix  $\mathbf{M} \in \mathbb{R}^{n \times p}$ , let  $\mathbf{m}_j$  and  $m_{ij}$ , respectively, denote the  $j$ -th column and  $(i, j)$  entry of  $\mathbf{M}$  for  $i = 1, \dots, n$  and  $j = 1, \dots, p$ . For any index set  $\mathcal{I} \subset \{1, \dots, p\}$ , let  $\mathbf{v}_{\mathcal{I}}$  and  $\mathbf{M}_{\mathcal{I}}$  denote the subvector of  $\mathbf{v}$  whose elements are indexed by  $\mathcal{I}$  and the submatrix of  $\mathbf{M}$  whose columns are indexed by  $\mathcal{I}$ , respectively. Let  $I(\mathcal{A})$  denote the indicator function of the event  $\mathcal{A}$ ; i.e.,  $I(\mathcal{A}) = 1$  if  $\mathcal{A}$  is true, and  $I(\mathcal{A}) = 0$  otherwise. Finally, we let  $\|\mathbf{v}\|_0 = \sum_{j=1}^p I(v_j \neq 0)$ ,  $\|\mathbf{v}\|_q = \left(\sum_{j=1}^p |v_j|^q\right)^{1/q}$  for any  $0 < q < \infty$ ,  $\|\mathbf{v}\|_\infty = \max_j |v_j|$ ,  $\|\mathbf{v}\|_{\mathbf{K}}^2 = \mathbf{v}^\top \mathbf{K} \mathbf{v}$  for any positive definite matrix  $\mathbf{K}$ ,  $\|\mathbf{M}\|_q = \sup_{\|\mathbf{v}\|_q=1} \|\mathbf{M}\mathbf{v}\|_q$  for any  $q > 0$  and  $\|\mathbf{M}\|_F^2 = \sum_{i=1}^n \sum_{j=1}^p m_{ij}^2$ .

## 2 The GMD Regression

We first briefly review the generalized matrix decomposition (GMD). The GMD of  $\mathbf{X}$  with respect to  $\mathbf{H}$  and  $\mathbf{Q}$ ,  $\mathbf{X} = \mathbf{U}\mathbf{S}\mathbf{V}^\top$ , is obtained by solving the following optimization problem:

$$\operatorname{argmin}_{\mathbf{U}, \mathbf{S}, \mathbf{V}} \|\mathbf{X} - \mathbf{U}\mathbf{S}\mathbf{V}^\top\|_{\mathbf{H}, \mathbf{Q}}, \quad (2)$$

subject to  $\mathbf{U}^\top \mathbf{H} \mathbf{U} = \mathbf{I}_K$ ,  $\mathbf{V}^\top \mathbf{Q} \mathbf{V} = \mathbf{I}_K$  and  $\mathbf{S} = \operatorname{diag}(\sigma_1, \dots, \sigma_K)$ . Here,  $K \leq \min(n, p)$  is the rank of  $\mathbf{X}^\top \mathbf{H} \mathbf{X} \mathbf{Q}$  and  $\|\mathbf{M}\|_{\mathbf{H}, \mathbf{Q}}^2 = \operatorname{tr}(\mathbf{M}^\top \mathbf{H} \mathbf{M} \mathbf{Q})$  for any matrix  $\mathbf{M} \in \mathbb{R}^{n \times p}$ . Note that unlike the SVD, the GMD vectors  $\mathbf{U}$  and  $\mathbf{V}$  are not orthogonal in the Euclidean norm unless  $\mathbf{H} = \mathbf{I}_n$  and  $\mathbf{Q} = \mathbf{I}_p$ . The GMD directly extends SVD by replacing the Frobenius norm with the  $\mathbf{H}, \mathbf{Q}$ -norm  $\|\cdot\|_{\mathbf{H}, \mathbf{Q}}$ . As such, GMD preserves appealing properties of SVD such as ordering the component vectors according to a nonincreasing set of GMD values,  $\sigma_1, \dots, \sigma_K$ , indicating that the decomposition of the total variance of  $\mathbf{X}$  into each dimension is nonincreasing. An efficient algorithm was proposed by Allen et al. (2014) to iteratively solve for each column of  $\mathbf{U}, \mathbf{S}$  and  $\mathbf{V}$  in (2). Analogous to the SVD of  $\mathbf{X}$ , which is closely related to the eigen-decomposition of  $\mathbf{X}^\top \mathbf{X}$ , the GMD of  $\mathbf{X}$  with respect to  $\mathbf{H}$  and  $\mathbf{Q}$  is related to the eigen-decomposition of  $\mathbf{X}^\top \mathbf{H} \mathbf{X} \mathbf{Q}$ . In fact, Escoufier (1987) and Allen et al. (2014) show that the squared GMD values  $\sigma_1^2, \dots, \sigma_K^2$  are non-zero eigenvalues of  $\mathbf{X}^\top \mathbf{H} \mathbf{X} \mathbf{Q}$ .

and columns of  $\mathbf{V}$  are the corresponding eigenvectors. Note that  $\mathbf{X}^T\mathbf{H}\mathbf{X}\mathbf{Q}$  may not be symmetric, again implying that columns of  $\mathbf{V}$  may not be orthogonal in the Euclidean norm. Given  $\mathbf{V}$  and  $\mathbf{S}$ , the  $n \times K$  matrix  $\mathbf{U}$  can be uniquely defined by  $\mathbf{U}\mathbf{S} = \mathbf{X}\mathbf{Q}\mathbf{V}$ .

To estimate  $\beta^*$  in (1), GMDR regresses  $\mathbf{y}$  on a reduced subset of GMD components. More specifically, let  $\nu_j = \mathbf{u}_j\sigma_j$  be the  $j$ -th GMD component for  $j = 1, \dots, K$  and set  $\Upsilon = [\nu_1 \cdots \nu_K] \in \mathbb{R}^{n \times K}$ . For any pre-determined index set  $\mathcal{I} \subset \{1, \dots, K\}$ , the GMDR estimator of  $\beta^*$ ,  $\hat{\beta}_{\text{GMDR}}(\mathcal{I})$ , can be obtained in two steps:

- (i) Regress  $\mathbf{y}$  on  $\Upsilon_{\mathcal{I}}$  and obtain  $\hat{\gamma}(\mathcal{I}) = \operatorname{argmin}_{\gamma} \|\mathbf{y} - \Upsilon_{\mathcal{I}}\gamma\|_{\mathbf{H}}^2$ .
- (ii) Calculate  $\hat{\beta}_{\text{GMDR}}(\mathcal{I}) = (\mathbf{Q}\mathbf{V})_{\mathcal{I}}\hat{\gamma}(\mathcal{I})$ .

Letting  $w_j = I(j \in \mathcal{I})$  for  $j = 1, \dots, K$ ,  $\hat{\beta}_{\text{GMDR}}(\mathcal{I})$  can be explicitly expressed as

$$\hat{\beta}_{\text{GMDR}}(\mathcal{I}) = \mathbf{Q}\mathbf{V}\mathbf{W}_{\mathcal{I}}\mathbf{S}^{-1}\mathbf{U}^T\mathbf{H}\mathbf{y}, \quad (3)$$

where  $\mathbf{W}_{\mathcal{I}} = \operatorname{diag}(w_1, \dots, w_K)$ .

It is critical to select the “best” index set  $\mathcal{I}$  that leads to the best prediction performance. First, if  $\mathbf{Q} = \mathbf{I}_p$  and  $\mathbf{H} = \mathbf{I}_n$ , then GMDR reduces to PCR. Thus, analogous to PCR, a natural way to select  $\mathcal{I}$  is to consider GMD components that correspond to large GMD values, referred to as top GMD components hereafter. However, there is a long historical debate on the rationale behind selecting top PCs for PCR because it is well known that, in general, top PCs are not necessarily more predictive of the outcome than tail PCs; see Cook (2007) and the references therein for more discussions.

A natural question arises: how to find the most predictive  $\mathcal{I}$  from all subsets of  $\{1, \dots, K\}$ ? Note that an exhaustive search over all  $2^K$  subsets of  $\{1, \dots, K\}$  is computationally infeasible even for moderate  $K$ . To address this problem, we propose a procedure that weighs the importance of each GMD component by its contribution to the prediction of the outcome. Our idea is to decompose the total  $R^2$  of the model into  $K$  terms, each corresponding to a GMD component. More specifically, we first regress  $\mathbf{y}$  on all GMD

components  $\mathbf{Y}$  with respect to the  $\mathbf{H}$ -norm, and obtain

$$\hat{\boldsymbol{\gamma}} = \operatorname{argmin}_{\boldsymbol{\gamma}} \|\mathbf{y} - \mathbf{Y}\boldsymbol{\gamma}\|_{\mathbf{H}}^2. \quad (4)$$

It can then be seen that the total  $R^2$  for the model is given by  $R^2 = \|\mathbf{Y}\hat{\boldsymbol{\gamma}}\|_{\mathbf{H}}^2 / \|\mathbf{y}\|_{\mathbf{H}}^2$ . Letting  $\hat{\boldsymbol{\gamma}} = (\hat{\gamma}_1, \dots, \hat{\gamma}_K)^\top$ , we can write  $R^2 = \sum_{j=1}^K r_j^2$ , where

$$r_j^2 = \frac{\|\boldsymbol{\nu}_j \hat{\gamma}_j\|_{\mathbf{H}}^2}{\|\mathbf{y}\|_{\mathbf{H}}^2} = \frac{\sigma_j^2 \hat{\gamma}_j^2}{\|\mathbf{y}\|_{\mathbf{H}}^2}, \text{ for } j = 1, \dots, K.$$

Here, we use the fact that  $\boldsymbol{\nu}_i^\top \mathbf{H} \boldsymbol{\nu}_j = 0$  for any  $i \neq j$ . Since  $r_1^2, \dots, r_K^2$  share the same denominator, we define the *variable importance* (VI) score of the  $j$ -th GMD component as  $\text{VI}_j = \sigma_j^2 \hat{\gamma}_j^2$  for  $j = 1, \dots, K$ , with a higher score being more predictive of the outcome.

Based on  $\text{VI}_1, \dots, \text{VI}_K$ , we select the most predictive  $\mathcal{I}$  in three steps:

- (i) Sort  $\{\text{VI}_j : j = 1, \dots, K\}$  in nonincreasing order:  $\text{VI}_{j_1} \geq \text{VI}_{j_2} \geq \dots \geq \text{VI}_{j_K}$ .
- (ii) For each  $k = 1, \dots, K$ , consider  $\mathcal{I}_k = \{j_1, \dots, j_k\}$  and calculate the generalized cross-validation (GCV) statistic:

$$\text{GCV}(k) = \frac{\|(\mathbf{I}_n - \mathbf{G}(k)) \mathbf{y}\|_{\mathbf{H}}^2}{(\text{tr}(\mathbf{I}_n - \mathbf{G}(k)))^2} = \frac{\|(\mathbf{I}_n - \mathbf{G}(k)) \mathbf{y}\|_{\mathbf{H}}^2}{(n - k)^2},$$

where  $\mathbf{G}(k) = \mathbf{Y}_{\mathcal{I}_k} (\mathbf{Y}_{\mathcal{I}_k}^\top \mathbf{H} \mathbf{Y}_{\mathcal{I}_k})^{-1} \mathbf{Y}_{\mathcal{I}_k}^\top \mathbf{H}$ .

- (iii) Find  $k_{opt} = \operatorname{argmin}_k \text{GCV}(k)$ , and obtain  $\mathcal{I}_{k_{opt}} = \{j_1, \dots, j_{k_{opt}}\}$ .

Having selected the most predictive GMD components, we now return to the estimation of regression coefficients. It can be seen from (3) that our GMDR estimator  $\hat{\boldsymbol{\beta}}_{\text{GMDR}}(\mathcal{I})$  belongs to the following class of estimators:

$$\mathcal{B}_{\text{GMD}} = \{\boldsymbol{\beta}^w \in \mathbb{R}^p : \boldsymbol{\beta}^w = \mathbf{Q}\mathbf{V}\mathbf{W}\mathbf{S}^{-1}\mathbf{U}^\top \mathbf{H}\mathbf{y}\} \quad (5)$$



for some weight matrix  $\mathbf{W} = \text{diag}(w_1, \dots, w_K)$ , where  $w_j \geq 0$  for  $j = 1, \dots, K$ . Besides selecting each  $w_j$  as either 0 or 1, as done for GMDR, one can instead let  $w_j$  depend on a tuning parameter  $\eta$ . For example, letting  $w_j = w_j(\eta) = (\sigma_j^2 + \eta)^{-2} \sigma_j^2$  and  $\mathbf{W}_\eta = \text{diag}(w_1(\eta), \dots, w_K(\eta))$ , one can obtain another estimator in  $\mathcal{B}_{\text{GMD}}$  as  $\boldsymbol{\beta}^w(\eta) = \mathbf{Q}\mathbf{V}\mathbf{W}_\eta\mathbf{S}^{-1}\mathbf{U}^\top\mathbf{H}\mathbf{y}$ . It can be show that (see the derivations in Section (A1) of the Appendix)

$$\boldsymbol{\beta}^w(\eta) = \underset{\boldsymbol{\beta}}{\text{argmin}} \left\{ \|\mathbf{y} - \mathbf{X}\boldsymbol{\beta}\|_{\mathbf{H}}^2 + \eta \|\boldsymbol{\beta}\|_{\mathbf{Q}^{-1}}^2 \right\} := \hat{\boldsymbol{\beta}}_{\text{KPR}}(\eta), \quad (6)$$

where  $\hat{\boldsymbol{\beta}}_{\text{KPR}}(\eta)$  is the estimator obtained from KPR (Randolph et al., 2018). Although the motivations behind KPR and GMDR are quite different, (6) implies that they share many features. First, both  $\hat{\boldsymbol{\beta}}_{\text{GMDR}}(\mathcal{I})$  and  $\hat{\boldsymbol{\beta}}_{\text{KPR}}(\eta)$  are in the column space of  $\mathbf{Q}$ , indicating both estimators incorporate information from  $\mathbf{Q}$  in similar ways. Second, both estimators exert shrinkage effects on the GMD components through the weight matrix  $\mathbf{W}$ . The difference is that,  $\hat{\boldsymbol{\beta}}_{\text{GMDR}}(\mathcal{I})$  exerts discrete shrinkage by truncation, nullifying the contribution of the GMD components that are not selected, while  $\hat{\boldsymbol{\beta}}_{\text{KPR}}(\eta)$  exerts a smooth shrinkage effect through the tuning parameter  $\eta$  inherently involved in its construction. This connection between GMDR and KPR is similar to that between PCR and the ridge regression (see Section 3.4 in Friedman et al. (2001) for more details).

### 3 The GMD Inference

In this section, we propose a high-dimensional inferential framework for the parameter of interest  $\boldsymbol{\beta}^*$ , called the GMD inference (GMDI), based on any arbitrary estimator in the class  $\mathcal{B}_{\text{GMD}}$ , given in (5). This inferential procedure and its theoretical properties are presented in Section 3.1. In Section 3.2, we provide additional explanations for the key assumptions made in Section 3.1. Recall from (1) that  $\mathbf{y} = \mathbf{X}\boldsymbol{\beta}^* + \boldsymbol{\epsilon}$ , where  $\mathbb{E}[\boldsymbol{\epsilon} \mid \mathbf{X}] = \mathbf{0}_n$  and  $\text{Cov}(\boldsymbol{\epsilon} \mid \mathbf{X}) = \boldsymbol{\Psi}$ . Letting  $\boldsymbol{\Psi} = \mathbf{L}_\psi^\top \mathbf{L}_\psi$ ,  $\boldsymbol{\epsilon} = \mathbf{L}_\psi^\top \tilde{\boldsymbol{\epsilon}}$  and  $\tilde{\boldsymbol{\epsilon}} = (\tilde{\epsilon}_1, \dots, \tilde{\epsilon}_n)^\top$ , we assume

that  $\tilde{\epsilon}_1, \dots, \tilde{\epsilon}_n$  are *i.i.d. sub-Gaussian* random variables with mean 0 and variance 1; that is, there exists a constant  $C > 0$  such that

$$\mathbb{E}[\exp(t\tilde{\epsilon}_i)] \leq \exp\left(\frac{Ct^2}{2}\right) \quad \text{for all } t \in \mathbb{R} \text{ and } i = 1, \dots, n. \quad (7)$$

Assumption (7) is less restrictive than the Gaussianity assumed in Bühlmann (2013) and Zhang and Zhang (2014). Nonetheless, sub-Gaussianity is only considered for ease of presentation; our results can be easily extended to other distributions with certain tail bounds, such as sub-exponential distributions (Chapter 2, Wainwright, 2019).

### 3.1 The GMDI Procedure

Let  $\boldsymbol{\beta}^w = (\beta_1^w, \dots, \beta_p^w)^\top$  be an arbitrary estimator from  $\mathcal{B}_{\text{GMD}}$  in (5) with an arbitrarily fixed weight matrix  $\mathbf{W}$ . Our goal is to test the null hypothesis  $H_{0,j} : \beta_j^* = 0$  for some  $j = 1, \dots, p$ . We first note that  $\beta_j^w$  can be a biased estimator of  $\beta_j^*$ . Letting  $B_j$  denote the bias of  $\beta_j^w$ , it can be seen that

$$B_j = (\mathbf{Q}\mathbf{V}\mathbf{W}\mathbf{V}^\top \boldsymbol{\beta}^*)_j - \beta_j^* = \sum_{m \neq j} \xi_{jm}^w \beta_m^* + (\xi_{jj}^w - 1)\beta_j^*,$$

where  $\xi_{jm}^w = (\mathbf{Q}\mathbf{V}\mathbf{W}\mathbf{V}^\top)_{(j,m)}$ , for  $j, m = 1, \dots, p$ . Under  $H_{0,j}$ , one can see that for any  $h_j \in \mathbb{R}$ ,

$$B_j = B_j(h_j) := \sum_{m \neq j} \xi_{jm}^w \beta_m^* + h_j(\xi_{jj}^w - 1)\beta_j^*.$$

To construct a test statistic for testing  $H_{0,j}$  based on  $\beta_j^w$ , we correct the bias  $B_j(h_j)$  using a consistent initial estimator of  $\boldsymbol{\beta}^*$ . Let  $\boldsymbol{\beta}^{init} = (\beta_1^{init}, \dots, \beta_p^{init})^\top$  denote such an initial estimator (we will discuss it in detail later in this section), we can estimate  $B_j(h_j)$  by

$$\hat{B}_j(h_j) = \sum_{m \neq j} \xi_{jm}^w \beta_m^{init} + h_j(\xi_{jj}^w - 1)\beta_j^{init}. \quad (8)$$

Then, our bias-corrected estimator of  $\beta_j^*$  is given by

$$\widehat{\beta}_j^w(h_j) = \beta_j^w - \widehat{B}_j(h_j), \quad j = 1, \dots, p. \quad (9)$$

**Remark 3.1.** Let  $\theta^*$  be the projection of  $\beta^*$  onto the column space of  $\mathbf{QV}$ . Similar to Shao and Deng (2012), when  $p > n$ ,  $B_j$  can be decomposed as the sum of the estimation and projection biases, given by  $(\mathbf{QVWV}^\top \beta^*)_j - \theta_j$  and  $\theta_j - \beta_j^*$ , respectively. Unlike Bühlmann (2013) that only corrects the projection bias, i.e.,  $\theta_j - \beta_j^*$ , our bias-corrected estimator in (9) provides tighter bias correction by correcting both the estimation and projection biases.

**Remark 3.2.** The two most intuitive choices of  $h_j$  are 0 and 1, which are, respectively, considered in Bühlmann (2013) and Zhao and Shojaie (2016). By considering  $h_j = 0$ , one only corrects the bias under the null hypothesis, while  $h_j = 1$  corrects the general bias regardless of  $\beta_j^*$ . While other choices of  $h_j$  are mathematically valid, they are practically less meaningful. Thus, we shall limit the following discussion to consider  $h_j = 0$  or 1.

The following result characterizes the asymptotic distribution of  $\widehat{\beta}_j^w(h_j)$  as  $n \rightarrow \infty$ .

**Proposition 3.1.** For  $j = 1, \dots, p$ , consider the bias-corrected estimator  $\widehat{\beta}_j^w(h_j)$ , given in (9). Letting  $a_{ji} = (\mathbf{QVWS}^{-1}\mathbf{U}^\top\mathbf{HL}_\psi^\top)_{(j,i)}$ , if

$$\lim_{n \rightarrow \infty} \frac{\max_{i=1, \dots, n} |a_{ji}|}{\sqrt{\sum_{i=1}^n a_{ji}^2}} = 0, \quad (10)$$

then for  $h_j \in \{0, 1\}$ ,

$$\widehat{\beta}_j^w(h_j) = ((1 - h_j)\xi_{jj}^w + h_j) \beta_j^* + \sum_{m \neq j} \xi_{jm}^w (\beta_m^* - \beta_m^{init}) + h_j (\xi_{jj}^w - 1) (\beta_j^* - \beta_j^{init}) + Z_j^w. \quad (11)$$

Here,  $Z_j = \sum_{i=1}^n a_{ji} \tilde{\epsilon}_i$  and

$$\frac{Z_j^w}{\sqrt{\Omega_{jj}^w}} \xrightarrow{d} N(0, 1) \text{ as } n \rightarrow \infty,$$

where

$$\Omega_{jj}^w = \{ \mathbf{QVWS}^{-1} \mathbf{U}^\top \mathbf{HL}_\psi^\top (\mathbf{QVWS}^{-1} \mathbf{U}^\top \mathbf{HL}_\psi^\top)^\top \}_{(j,j)}.$$

An immediate consequence of this result is that if  $\boldsymbol{\beta}^{init}$  is a consistent estimator of  $\boldsymbol{\beta}^*$ , i.e.,  $\|\boldsymbol{\beta}^* - \boldsymbol{\beta}^{init}\|_1 = o_p(1)$  as  $n \rightarrow \infty$ , and  $\mathbf{L}_\psi$  can be consistently estimated, then with  $\mathbf{L}_\psi$  replaced by its estimate,  $\left| (\Omega_{jj}^w)^{-1/2} \widehat{\beta}_j^w(h_j) \right|$  is an asymptotically valid test statistic for testing  $H_{0,j}$ . Existing HDI tools that also perform bias-correction use the lasso estimator (Tibshirani, 1996) as the initial estimator (Bühlmann, 2013; Zhao and Shojaie, 2016). Consistency of the lasso estimator requires that (i) the true regression coefficient vector is sparse, and (ii) the design matrix satisfies a restricted eigenvalue-type condition (van de Geer et al., 2009). However, for two-way structured regression, due to potential strong correlations among variables, the true coefficients in two-way structured regression may not be sparse, and any restricted eigenvalue-type condition may fail (see van de Geer et al. (2009) for more discussions). For estimation of the variance component  $\mathbf{L}_\psi$  in high-dimensional settings, most existing methods consider the case that  $\mathbf{L}_\psi = \sigma^2 \mathbf{I}_n$ ; i.e., the samples are assumed to be *i.i.d.* (Reid et al., 2016; Yu and Bien, 2019). As such, the problem of estimating  $\mathbf{L}_\psi$  reduces to estimating  $\sigma^2$ . However, this simple covariance structure may be limited because samples are likely to be dependent and heteroscedastic for two-way structured data.

To overcome these difficulties, we assume that the auxiliary information  $\mathbf{H}$  and  $\mathbf{Q}$  inform the structure of  $\mathbf{L}_\psi$ ,  $\boldsymbol{\beta}^*$  and  $\mathbf{X}$  in certain ways. More specifically, the first assumption states that  $\mathbf{H}$  informs  $\mathbf{L}_\psi$  in terms of the spectral norm of  $\mathbf{L}_\psi \mathbf{H} \mathbf{L}_\psi^\top$ .

$$(A1) \text{ As } n \rightarrow \infty, \|\mathbf{L}_\psi \mathbf{H} \mathbf{L}_\psi^\top - \mathbf{I}_n\|_2 = o(1).$$

A stronger assumption than Assumption (A1) is that  $\mathbf{H} = (\mathbf{L}_\psi^\top \mathbf{L}_\psi)^{-1} = \boldsymbol{\Psi}^{-1}$ . Compared to this stronger assumption, Assumption (A1) is more flexible because it only requires that  $\mathbf{H}$  is close to  $\boldsymbol{\Psi}^{-1}$  in the sense that the spectral norm of  $\mathbf{L}_\psi \mathbf{H} \mathbf{L}_\psi^\top$  is close to 1. Here, we assume  $\mathbf{H}$  directly informs  $\boldsymbol{\Psi}^{-1}$ , not  $\boldsymbol{\Psi}$ , because we have assumed in Section 1.1 that  $\mathbf{H}$  informs the *conditional* similarities between samples. It is well-known that such conditional

similarities can be characterized by partial correlations, which are closely related to the inverse covariance matrix. The following proposition states that if Assumption (A1) holds, then  $Z_j^w$  (see Proposition 3.1) converges in distribution to  $N(0, R_{jj}^w)$  as  $n \rightarrow \infty$ , where  $R_{jj}^w = \{\mathbf{Q}\mathbf{V}\mathbf{W}^2\mathbf{S}^{-2}\mathbf{V}^\top\mathbf{Q}\}_{(j,j)}$ .

**Proposition 3.2.** *Consider the  $Z_j^w$  defined in Proposition 3.1. Suppose that Assumption (A1) and condition (10) hold. Then, we have*

$$\frac{Z_j^w}{\sqrt{R_{jj}^w}} \xrightarrow{d} N(0, 1) \text{ as } n \rightarrow \infty.$$

The proofs of Propositions 3.1 and 3.2 are given in Section (A2) of the Appendix.

Unlike existing HDI procedures which assume the sparsity of  $\boldsymbol{\beta}^*$ , we assume that  $\boldsymbol{\beta}^*$  is informed by the eigenvectors of  $\mathbf{Q}$ . Roughly speaking, we assume that the majority of the signals in  $\boldsymbol{\beta}^*$  can be captured by a few eigenvectors of  $\mathbf{Q}$ . Specifically, denoting by  $\mathbf{Q} = \mathbf{D}\boldsymbol{\Delta}\mathbf{D}^\top$  the eigen-decomposition of  $\mathbf{Q}$  and  $\tilde{\boldsymbol{\beta}}^* = \mathbf{D}^\top\boldsymbol{\beta}^*$ , we assume

(A2) For some  $S_0 \subset \{1, \dots, p\}$  with  $s_0 = |S_0|$ ,  $\|\tilde{\boldsymbol{\beta}}_{S_0^c}^*\|_1 \leq \eta_1$ , where

$$\eta_1 = O\left(\sqrt{n^{-1}s_0 \log p}\right) \text{ and } s_0 = o\left\{(n/\log p)^r\right\} \text{ for some } r \in (0, 1/2)$$

as  $n \rightarrow \infty$ .

Under Assumption (A2),  $\|\boldsymbol{\beta}^*\|_{\mathbf{Q}^{-1}}$ , the penalty term of KPR (see (6)), is likely to be small. Thus, Assumption (A2) is in fact aligned with the key idea of KPR. Also, in Section 3.2, we will show that any estimator from the class  $\mathcal{B}_{\text{GMD}}$  is less biased if  $\boldsymbol{\beta}^*$  satisfies Assumption (A2).

Our third assumption characterizes how  $\mathbf{H}$  and  $\mathbf{Q}$ , respectively, inform the row and column structures of the design matrix  $\mathbf{X}$ . As mentioned earlier, any restricted eigenvalue-type condition may break down due to potentially strong correlations in  $\mathbf{X}$ . We assume that  $\mathbf{H}$  and  $\mathbf{Q}$  can help decorrelate the rows and columns of  $\mathbf{X}$ , respectively, so that the

decorrelated design matrix satisfies a restricted eigenvalue-type condition. More specifically, we assume

(A3) For some constants  $0 < c_* < c^* < \infty$ ,

$$c_* \leq \frac{\|\check{\mathbf{X}}_A \mathbf{v}\|^2}{n \|\mathbf{v}\|^2} \leq c^* \quad \text{for any } A \subset \{1, \dots, p\} \text{ with } |A| = q^* \text{ and } \mathbf{v} \in \mathbb{R}^*,$$

where  $\check{\mathbf{X}} = \mathbf{H}^{1/2} \mathbf{X} \mathbf{D} \mathbf{\Delta}^{1/2}$ ,  $q^* \geq M_1^* s_0 + 1$  with  $s_0$  given in Assumption (A2) and  $M_1^*$  specified in Section (A3) of the Appendix.

Letting  $\check{\Sigma}_A = n^{-1} \check{\mathbf{X}}_A^\top \check{\mathbf{X}}_A$ , Assumption (A3) implies that all eigenvalues of  $\check{\Sigma}_A$  are inside the interval  $[c_*, c^*]$  when the size of  $A$  is no greater than  $q^*$ . This assumption is called the sparse Riesz condition (Zhang et al., 2008). According to Proposition 1 in Zhang et al. (2008), if there exists some  $q^*$  such that the maximum correlation between the variables in  $\check{\mathbf{X}}$  is bounded by  $\delta/(q^* - 1)$  for some  $\delta < 1$ , then this condition holds with rank  $q^*$ ,  $c_* = 1 - \delta$  and  $c^* = 1 + \delta$ .

Under assumptions (A1)–(A3), we construct  $\beta^{init}$  in two steps:

(i) Find

$$\tilde{\beta}(\lambda) = \operatorname{argmin}_{\beta} \left\{ \frac{1}{2} \|\mathbf{y} - \mathbf{X} \mathbf{D} \beta\|_{\mathbf{H}}^2 + \lambda \|\mathbf{\Delta}^{-1/2} \beta\|_1 \right\}. \quad (12)$$

(ii) Define  $\beta^{init} = \mathbf{D} \tilde{\beta}(\lambda)$ .

Here,  $\lambda > 0$  is a tuning parameter. We use a weighted  $l_1$  penalty in (12) with the weights equal to the inverse of the square root of the eigenvalues of  $\mathbf{Q}$ . We will explain the rationale behind this choice of weights in Section 3.2.

Letting  $\zeta_j(h_j) = \sum_{m \neq j} \xi_{jm}^w (\beta_m^* - \beta_m^{init}) + h_j (\xi_{jj}^w - 1) (\beta_j^* - \beta_j^{init})$  for  $j = 1, \dots, p$  and  $\Xi = \operatorname{diag}(\xi_{11}^w, \dots, \xi_{pp}^w)$ , the following result serves as the basis for constructing an asymptotically valid test for  $H_{0,j}$  using the bias-corrected estimator  $\hat{\beta}_j^w(h_j)$  given in (11). In the following theorems, without loss of generality, we assume that  $\mathbf{Q}$  is appropriately scaled such that  $\|\mathbf{Q}\|_2 = 1$ .

**Theorem 3.1.** *Suppose the columns of  $\mathbf{X}$  are standardized such that  $\|\mathbf{X}\mathbf{d}_j\|_{\mathbf{H}}^2 = n$ , where  $\mathbf{d}_j$  is the  $j$ -th column of  $\mathbf{D}$  for  $j = 1, \dots, p$ . For  $\tilde{\boldsymbol{\beta}}(\lambda)$  in (12), consider*

$$\lambda = 2\sqrt{2c^*n \log p(1 + c_0)\|\mathbf{L}_\psi^\top \mathbf{H} \mathbf{L}_\psi\|_2}$$

with any  $c_0 > 0$ , where  $c^*$  is given in Assumption (A3). For  $h_j \in \{0, 1\}$ , denote

$$\Psi_j(h_j) = \left\| [(\mathbf{Q}\mathbf{V}\mathbf{W}\mathbf{W}^\top - (1 - h_j)\boldsymbol{\Xi} - h_j\mathbf{I}_p)\mathbf{D}]_{(j,\cdot)} \right\|_\infty \left( \frac{\log p}{n} \right)^{1/2-r},$$

where for any matrix  $\mathbf{M}$ ,  $\mathbf{M}_{(j,\cdot)}$  denotes the  $j$ -th row of  $\mathbf{M}$ . Then, under condition (10) and Assumptions (A1)–(A3), we have  $\lim_{n \rightarrow \infty} \Pr(|\zeta_j(h_j)| \leq \Psi_j(h_j)) = 1$ . Furthermore, under  $H_{0,j}$ , for any  $\alpha > 0$ ,

$$\limsup_{n \rightarrow \infty} \Pr\left(\left|\widehat{\beta}_j^w(h_j)\right| > \alpha\right) \leq \limsup_{n \rightarrow \infty} \Pr\left(|Z_j^w| + \Psi_j(h_j) > \alpha\right), \quad (13)$$

where  $Z_j^w$  is given in Proposition 3.1.

Combining Theorem 3.1 with Proposition 3.2, we can test  $H_{0,j}$  using the asymptotically valid two-sided  $p$ -value

$$P_j^w(h_j) = 2 \left\{ 1 - \Phi \left( (R_{jj}^w)^{-1/2} \left\{ \left| \widehat{\beta}_j^w(h_j) \right| - \Psi_j(h_j) \right\}_+ \right) \right\}, \quad (14)$$

where  $\Phi(\cdot)$  is the cumulative distribution function of the standard normal distribution and  $a_+ = \max(a, 0)$ .

Our next result guarantees the power of GMDI when the size of the true regression coefficient is sufficiently large.

**Theorem 3.2.** *Assume the conditions in Theorem 3.1 hold. For  $h_j \in \{0, 1\}$ , if there exists*

some  $0 < \alpha < 1$  and  $0 < \psi < 1$  such that

$$|\beta_j^*| \geq |(1 - h_j)\xi_{jj}^w + h_j|^{-1} \left( 2\Psi_j(h_j) + (q_{(1-\alpha/2)} + q_{(1-\psi/2)}) \sqrt{R_{jj}^w} \right), \quad (15)$$

where  $\Phi(q_t) = t$  for any  $t \in (0, 1)$ , then

$$\lim_{n \rightarrow \infty} \Pr(P_j^w(h_j) \leq \alpha) \geq \psi.$$

It should be noted that condition (15) cannot hold when  $h_j = 0$  and  $\xi_{jj}^w = 0$ ; however, this rarely happens and can be easily checked in advance. In cases where (15) is not true,  $h_j = 1$  can be used. Proofs of Theorems 3.1 and 3.2 are provided in Appendix (A3) and (A4), respectively.

### 3.2 Further Explanation of GMDI Assumptions

In this section, we provide additional rationale for Assumptions (A2) and the weighted  $l_1$  penalty used in (12) from the perspective of the bias of any arbitrary estimator in  $\mathcal{B}_{\text{GMD}}$ .

Recall that the bias of  $\beta^w = \mathbf{Q}\mathbf{V}\mathbf{W}\mathbf{S}^{-1}\mathbf{U}^\top\mathbf{H}\mathbf{y}$  is given by

$$\text{Bias}(\beta^w) = \mathbb{E}(\beta^w) - \beta^* = \mathbf{Q}\mathbf{V}\mathbf{W}\mathbf{V}^\top\beta^* - \beta^*. \quad (16)$$

We can rewrite (16) as

$$\text{Bias}(\beta^w) = \mathbf{Q}(\mathbf{V}\mathbf{W}\mathbf{V}^\top\mathbf{Q} - \mathbf{I}_p)\mathbf{Q}^{-1}\beta^*. \quad (17)$$

Recalling  $K = \text{rank}(\mathbf{X}\mathbf{Q}\mathbf{X}^\top\mathbf{H})$ , we make the following observations from (17).

- (O1) Suppose  $K = p$ . Let  $\beta^w$  be the GMDR estimator with all GMD components selected. In this case,  $\mathbf{W} = \mathbf{I}_p$  and it can be seen that  $\mathbf{V}\mathbf{W}\mathbf{V}^\top\mathbf{Q} = \mathbf{I}_p$ . Thus,  $\text{Bias}(\beta^w) = 0$ . This demonstrates that in the low-dimensional case ( $K = p \leq n$ ), the GMDR



estimator based on all GMD components is an unbiased estimator of  $\boldsymbol{\beta}^*$  for any  $\boldsymbol{\beta}^* \in \mathbb{R}^p$ .

(O2) Suppose  $K < p$ , a common scenario in high-dimensional settings ( $n < p$ ). In this case, it can be seen that  $\mathbf{V}\mathbf{W}\mathbf{V}^\top\mathbf{Q} \neq \mathbf{I}_p$  for any weight matrix  $\mathbf{W}$ . Then, using (17), we have

$$\|\text{Bias}(\boldsymbol{\beta}^w)\|_2 \leq \|\mathbf{Q}\|_2 \|\mathbf{V}\mathbf{W}\mathbf{V}^\top\mathbf{Q} - \mathbf{I}_p\|_2 \|\mathbf{Q}^{-1}\boldsymbol{\beta}^*\|_2,$$

indicating that  $\boldsymbol{\beta}^w$  is less biased if  $\|\mathbf{Q}^{-1}\boldsymbol{\beta}^*\|_2$  is small. Since  $\mathbf{Q} = \mathbf{D}\boldsymbol{\Delta}\mathbf{D}^\top$ , it can be seen that

$$\|\mathbf{Q}^{-1}\boldsymbol{\beta}^*\|_2^2 = \sum_{j=1}^p \delta_j^{-2} (\mathbf{d}_j^\top \boldsymbol{\beta}^*)^2, \quad (18)$$

where  $\mathbf{d}_j$  is the  $j$ -th column of  $\mathbf{D}$ , i.e., the  $j$ -th eigenvector of  $\mathbf{Q}$ . Since  $\delta_1 \geq \dots \geq \delta_p > 0$ , (18) implies that  $\boldsymbol{\beta}^w$  is less biased if (i) only a few  $|\mathbf{d}_j^\top \boldsymbol{\beta}^*|$  are non-zero, and (ii) for large  $j$  (small  $\delta_j$ ),  $\mathbf{d}_j^\top \boldsymbol{\beta}^* = 0$ . Since Assumption (A2) indicates that the majority of the signals in  $\boldsymbol{\beta}^*$  lie in the space spanned by a few eigenvectors of  $\mathbf{Q}$ , it aligns well with (i). The weighted  $l_1$  penalty in (12) encourages  $\mathbf{d}_j^\top \boldsymbol{\beta}^*$  to be 0 for large  $j$  and thus aligns with (ii).

## 4 Simulation Studies

We conducted two simulation studies, each containing multiple settings to compare the proposed GMDI with five existing high-dimensional inferential procedures: (i) the low-dimensional projection estimator (LDPE, Zhang and Zhang, 2014); (ii) the Ridge-based high-dimensional inference (Ridge, Bühlmann, 2013); (iii) the de-correlated score test (dscore, Ning and Liu, 2017); (iv) inference for the graph-constrained estimator (Grace, Zhao and Shojaie, 2016) and (v) the non-sparse high-dimensional inference (ns-hdi, Zhu and Bradic, 2018). In the first study, we simulated the two-way structured data from a matrix variate normal distribution with pre-specified row and column covariances. In the second study,

we performed data-driven simulations using a real microbiome data set. For both studies, we considered a two-sided significance level  $\alpha = 0.05$  for all the aforementioned tests.

As GMDI is proposed for the entire family of estimators  $\mathcal{B}_{\text{GMD}}$ , we considered two specific estimators from  $\mathcal{B}_{\text{GMD}}$ : (i) the proposed GMDR estimator in (3) and (ii) the KPR estimator in (6). We denote the resulting tests for the GMDR and KPR estimators by GMDI-d and GMDI-k respectively, because GMDR exerts *discrete* shrinkage effects on GMD components, whereas KPR exerts continuous shrinkage effects through a *kernel* function. For the selection of the index set  $\mathcal{I}$  of the GMDR estimator  $\hat{\boldsymbol{\beta}}_{\text{GMDR}}(\mathcal{I})$ , GMD components that explain less than 1% of the total variance are excluded because the estimated coefficients corresponding to the GMD components with low variances may be unstable. To see this, recall from (4) that  $\hat{\boldsymbol{\gamma}} = \operatorname{argmin}_{\boldsymbol{\gamma}} \|\mathbf{y} - \mathbf{Y}\boldsymbol{\gamma}\|_{\mathbf{H}}^2$ . Then,  $\hat{\gamma}_l = \sigma_l^{-1} \mathbf{u}_l^{\top} \mathbf{H} \mathbf{y}$  and  $\operatorname{Var}(\hat{\gamma}_l) = \sigma_c^2 \sigma_l^{-2}$ , for  $l = 1, \dots, K$ . This indicates that when the total  $R^2$  is low ( $\sigma_c^2$  is relatively large), for large  $l$  (small  $\sigma_l$ ),  $\hat{\gamma}_l$  may be unstable due to its large variance. The index set  $\mathcal{I}$  is then selected by the proposed GCV procedure based on the remaining GMD components. For the KPR estimator  $\hat{\boldsymbol{\beta}}_{\text{KPR}}(\eta)$ , the tuning parameter  $\eta$  is selected by 10-fold cross validation. For GMDI, the bias-correction parameter  $h_j$  (see Proposition 3.1) is set to be 1 for all  $j$ , as done for Grace; the tuning parameter  $\lambda$  in (12) is set to be  $2\sqrt{3n \log p}$ , and the sparsity parameter  $r$  is set to be 0.05. For LDPE and Ridge, we use the implementation in the R package `hdi`, and for the Grace test, we used the implementation in the R package `grace`. For LDPE, Ridge and Grace, the tuning parameters are selected using 10-fold cross validation.

## 4.1 Simulation I

We considered three settings in this study. In Settings I and II, we considered data with column structures, and examined how different choices of  $\mathbf{Q}$  may affect the performance of GMDI. In Setting III, we assessed the influence of sample (row) structure on all aforementioned inferential procedures.

**Setting I:** We first simulated  $\mathbf{X} \in \mathbb{R}^{200 \times 300}$  from a matrix variate normal distribution with mean  $\mathbf{0}$ , row covariance  $\mathbf{I}_{200}$  and column covariance  $\Sigma^{-1}$ , where

$$\Sigma_{(i,j)} = \begin{cases} 1, & i = j \\ 0.9^{|i-j|}, & i \neq j, i \leq 150, j \leq 150 \\ 0.5^{|i-j|}, & i \neq j, i > 150, j > 150 \\ 0, & \text{otherwise.} \end{cases}$$

Letting  $\mathbf{f}_j$  denote the  $j$ -th eigenvector of  $\Sigma$ , for  $j = 1, \dots, 300$ , we define  $\beta^* = \sum_{j=1}^{10} j^{-1/2} \mathbf{f}_j$ . Then, the outcome  $\mathbf{y}$  was generated according to  $\mathbf{y} = \mathbf{X}\beta^* + \epsilon$ , where  $\epsilon$  was simulated from a multivariate normal distribution with mean  $\mathbf{0}$  and covariance  $\Psi = \sigma_\epsilon^2 \mathbf{I}_{200}$ , and  $\sigma_\epsilon^2$  is selected to achieve an  $R^2$  of 0.4, 0.6 or 0.8.

Our GMDI was implemented with respect to  $\mathbf{H} = \sigma_\epsilon^{-2} \mathbf{I}_{200}$  and  $\mathbf{Q} = \Sigma$ . In this case, one can check that Assumption (A1) holds with  $\mathbf{H} = \Psi^{-1}$ , and Assumption (A2) holds with  $S_0 = \{1, \dots, 10\}$ . Also, with the selected  $\mathbf{H}$  and  $\mathbf{Q}$ , the transformed data matrix  $\tilde{\mathbf{X}}$  (see Assumption (A3) for its definition) follows a matrix variate normal distribution with diagonal row and column covariance matrices, indicating that Assumption (A3) holds with high probability. By design, the first 150 coefficients of  $\beta^*$  are non-zero, while the rest are zero. This enables us to evaluate the power from testing the non-zero coefficients and the type-I error rate from testing the zero coefficients.

The results are summarized in Fig. 1. Inspecting the type-I error of the tests in Fig. 1A shows that all methods but ns-hdi can (asymptotically) control the type-I error rate. This is likely because in this setting, the precision matrix of the variables,  $\Sigma$ , does not satisfy the row sparsity condition required by ns-hdi. Checking the power of the tests in Fig. 1B shows that both GMDI-k and GMDI-d have considerably higher power than the existing methods. More specifically, LDPE, Ridge and dscore have very low power since they completely ignore the column structure of  $\mathbf{X}$  and the non-sparsity of  $\beta^*$ . Because the Grace estimator correctly handles the column structure (Grace is implemented using

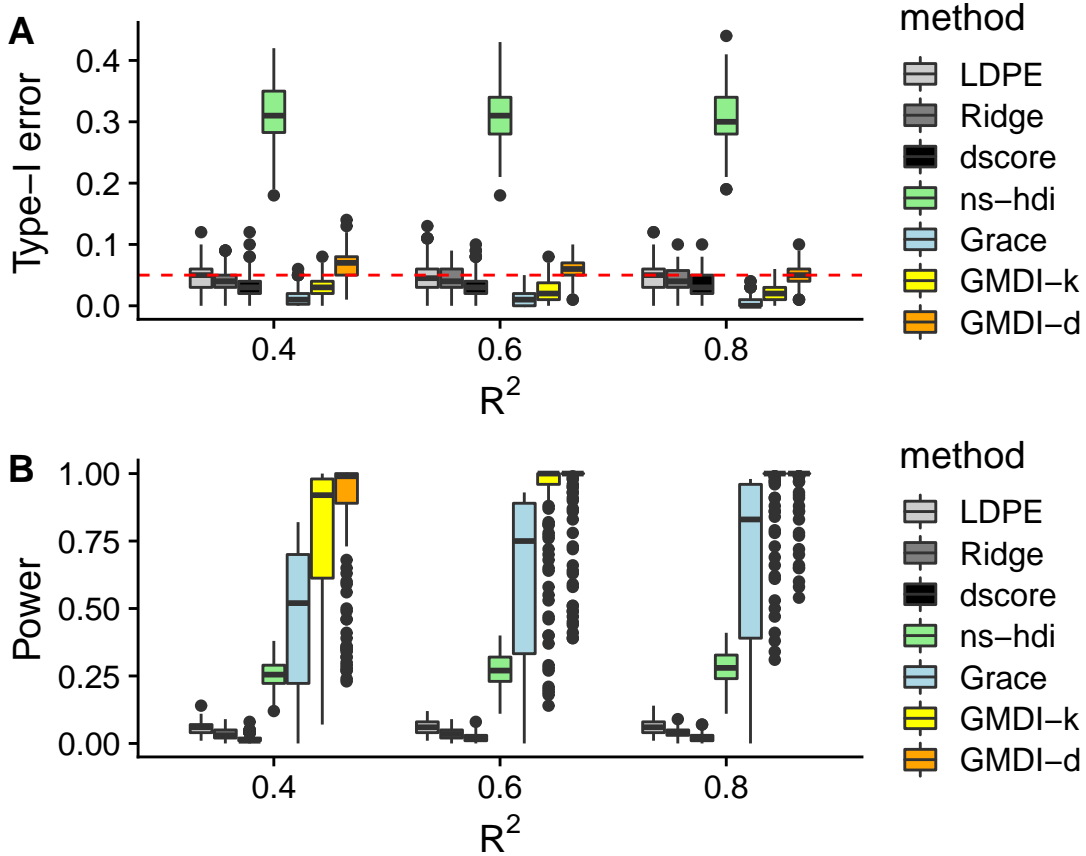


Figure 1: Boxplots of the type-I error (A) and power (B) over 500 replications for Setting I with  $R^2 = 0.4, 0.6$  and  $0.8$  : Both GMDI-d and GMDI-k can (asymptotically) control the type-I error, and have considerably higher power than other methods.

$\mathbf{L} = \Sigma^{-1}$ ; see see Zhao and Shojaie, 2016 for details), the Grace test gains more power than LDPE and Ridge. However, since the Grace test still requires the sparsity of  $\beta^*$ , which is not satisfied in this setting, it is not as powerful as GMDI-d or GMDI-k. These results clearly demonstrate the importance of incorporating informative column structures for gaining more power. As  $R^2$  increases, GMDI-k and GMDI-d both yield more stringent control of the type-I error and more power at the same time. GMDI-d has higher power than GMDI-k

especially for low  $R^2$  values; this is accompanied by the observation that GMDI-k yields more conservative control of the type-I error rate than GMDI-d. This difference between GMDI-d and GMDI-k may be attributed to the fact that GMDI-k shrinks all components, whereas GMDI-d only selects a subset of components without adding any shrinkage effect. Both GMDI-d and GMDI-k lead to some outliers with relatively low power. This is possibly due to less optimal selection of GMD components and tuning parameter for GMDI-d and GMDI-k, respectively.

**Setting II:** In the previous setting, our GMDI was implemented with respect to fully informative  $\mathbf{H}$  and  $\mathbf{Q}$ . In practice, one may not have correctly specified structural information. Thus, in this setting, we examined how different choices of  $\mathbf{Q}$  affect the performance of GMDI. The simulation setting is mostly the same as in Setting I except that instead of using  $\Sigma$  as  $\mathbf{Q}$ , we considered two perturbed matrices:  $\mathbf{Q}^{(1)}$  and  $\mathbf{Q}^{(2)}$ . Here,  $\mathbf{Q}^{(1)}$  is defined similar to  $\Sigma$ , except that  $\mathbf{Q}_{(i,j)}^{(1)} = 0.1^{|i-j|}$  for all  $(i, j) \in \{(a, b) : (a - 150)(b - 150) < 0\}$ , and  $\mathbf{Q}_{(i,j)}^{(2)} = 0.6^{|i-j|}$  for all  $i, j = 1, \dots, 300$ . One can check that Assumption (A2) roughly holds for  $\mathbf{Q}^{(1)}$ , but is completely violated for  $\mathbf{Q}^{(2)}$ . Thus,  $\mathbf{Q}^{(1)}$  and  $\mathbf{Q}^{(2)}$  are, respectively, an example of partially informative and non-informative auxiliary column structure. Only the results of Grace, GMDI-d and GMDI-k for  $R^2 = 0.6$  are summarized in Fig. 2, since other methods are not affected by the choice of  $\mathbf{Q}$ . Comparing Fig. 2 with Fig. 1, it can be seen that when  $\mathbf{Q}$  is partially informative i.e.,  $\mathbf{Q}^{(1)}$ , all the three methods can still (asymptotically) control the type-I error, but the power is compromised in each case due to this misspecification. When  $\mathbf{Q}$  is non-informative, i.e.,  $\mathbf{Q}^{(2)}$ , GMDI-d suffers from some inflation of the type-I error, while both Grace and GMDI-k seem to still control the type-I error. However, in other settings, when  $\mathbf{Q}$  is completely non-informative, we find that no methods can control the type-I error rate. See the discussions in Section 6 for a robust approach for choosing the appropriate structure among various auxiliary information.

**Setting III:** Next we assessed the effect of sample (row) structure in addition to the

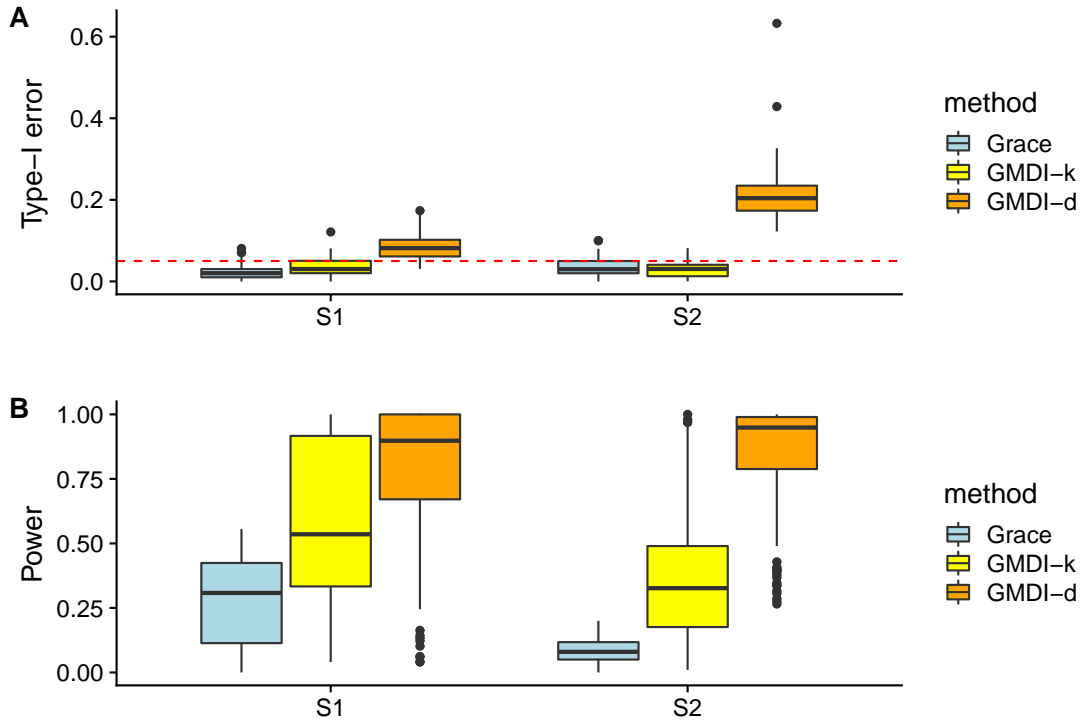


Figure 2: Boxplots of the type-I error (A) and the power (B) over 500 replications for Setting II with  $R^2 = 0.6$ . The S1 and S2 on the x-axis represent  $\mathbf{Q}^{(1)}$  and  $\mathbf{Q}^{(2)}$  respectively: Both GMDI-d and GMDI-k work well under small perturbations of  $\mathbf{Q}$ , but GMDI-d suffer more than GMDI-k from completely misspecified  $\mathbf{Q}$ .

column structure. Consider

$$\mathbf{R}_{(i,j)} = \begin{cases} 1, & i = j \\ 0.9^{|i-j|}, & i \neq j, i \leq 100, j \leq 100 \\ 0.5^{|i-j|}, & i \neq j, i > 100, j > 100 \\ 0, & \text{otherwise.} \end{cases}$$

We simulated  $\mathbf{X}$  from the matrix variate normal distribution with mean  $\mathbf{0}$ , row covariance  $\mathbf{R}^{-1}$  and column covariance  $\mathbf{\Sigma}^{-1}$ , where  $\mathbf{\Sigma}$  is defined in Setting I. Finally, using the same  $\boldsymbol{\beta}^*$  as in Setting I, we simulated the outcome  $\mathbf{y}$  by  $\mathbf{y} = \mathbf{X}\boldsymbol{\beta}^* + \boldsymbol{\epsilon}$ , where  $\boldsymbol{\epsilon}$  follows a multivariate normal distribution with mean  $\mathbf{0}$  and covariance  $\mathbf{R}^{-1}$ . The GMDI was implemented with respect to  $\mathbf{Q} = \mathbf{\Sigma}$  and three choices of  $\mathbf{H}$ :  $\mathbf{R}$ ,  $\mathbf{H}^{(1)}$  and  $\mathbf{I}_{200}$ . Here,  $\mathbf{H}^{(1)}$  is defined similar to  $\mathbf{R}$  except that  $\mathbf{H}_{(i,j)}^{(1)} = 0.1^{|i-j|}$  for all  $(i, j) \in \{(a, b) : (a - 100)(b - 100) < 0\}$ . One can check that Assumption (A1) holds when  $\mathbf{H} = \mathbf{R}$  and holds approximately when  $\mathbf{H} = \mathbf{H}^{(1)}$ , but is completely violated when  $\mathbf{H} = \mathbf{I}_{200}$ . The results are summarized in Fig. 3. All the existing methods, to varying degrees, fail to differentiate non-zero coefficients from zero ones. This is because these methods assume *i.i.d* samples, which is violated in this setting. In particular, the dscore test can control the type-I error in Setting I, whereas it fails in this setting with correlated samples. Also, the Grace test performs slightly better thanks to incorporating the column structure, but compared to Fig. 1B, its power is comprised due to ignoring the correlated samples. For the proposed GMDI, when  $\mathbf{H}$  is fully or partially informative, e.g.,  $\mathbf{H} = \mathbf{R}$  or  $\mathbf{H}^{(1)}$ , both GMDI-d and GMDI-k control the type-I error rate and have considerably higher power than the existing methods that control the type-I error. However, when  $\mathbf{H}$  is completely non-informative, both GMDI-d and GMDI-k suffer from a large inflation of the type-I error. These results demonstrate the importance of incorporating informative row structures.

## 4.2 Simulation II

In this study, we performed data-driven simulations using data collected as part of the “Carbohydrates and Related Biomarkers” (CARB) study, conducted between June 2006 and July 2009 at the Fred Hutchinson Cancer Research Center. This was a randomized, controlled, crossover feeding study aimed at evaluating the effects of glycemic load on a variety of biomarkers, such as systemic inflammation, insulin resistance, and adipokines (Neuhouser et al., 2012). Participants were randomized based on body mass index and

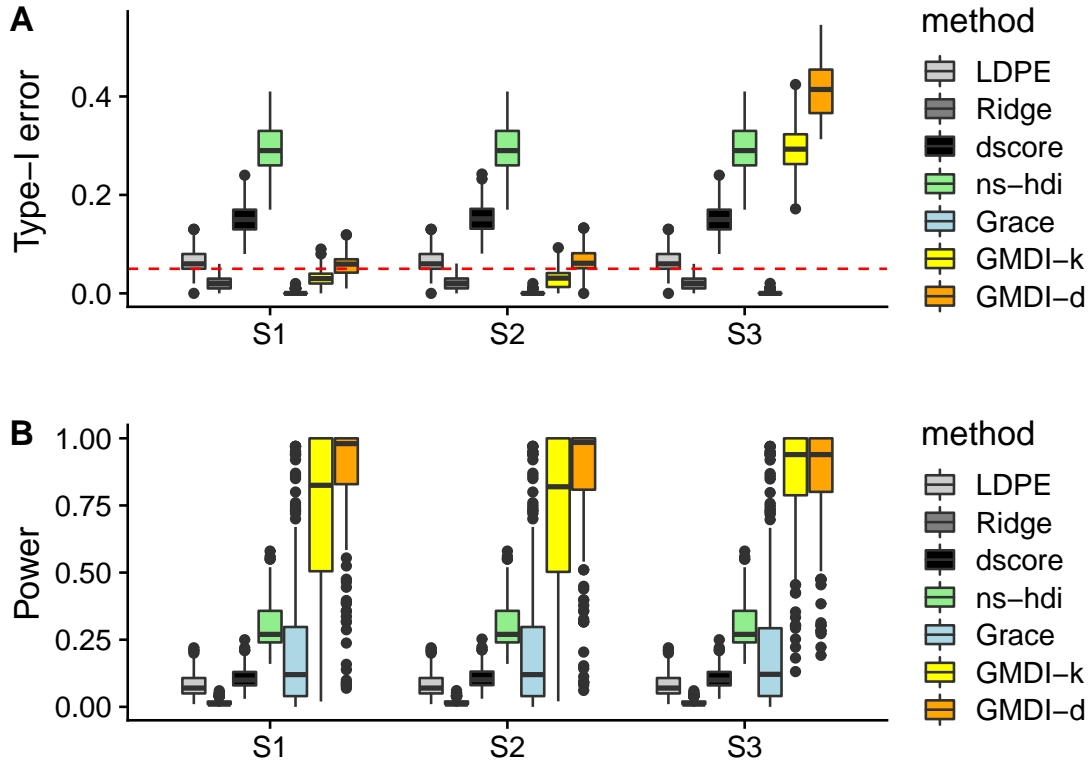


Figure 3: Boxplots of the type-I error (A) and power (B) over 500 replications for Setting III with  $R^2 = 0.6$ : (S1):  $\mathbf{H} = \mathbf{R}$ ; (S2):  $\mathbf{H} = \mathbf{H}^{(1)}$  and (S3):  $\mathbf{H} = \mathbf{I}_{200}$ . Both GMDI-d and GMDI-k show robustness with respect to small perturbations of  $\mathbf{H}$ , but neither can control the type-I error when  $\mathbf{H}$  is completely misspecified.

sex and fed two controlled diets (randomly assigned order) for 28 days, with a 28-day washout period between diets. The 16S rRNA genus abundance data used here are from 58 participants sampled at each of the three timepoints, resulting in 174 observations. To classify bacterial taxonomy, sequences were processed using QIIME (Caporaso et al., 2010). This processing produced a complete phylogenetic tree with 1054 leaves corresponding to level-7 taxa (species) defined by 97% similarity and 151 genera (level 6 of the tree). Our simulation used 114 genera after filtering out those that did not appear in at least 30% of



the 174 samples. We correspondingly trimmed the tree back to the genus level with 114 leaves.

Let  $\mathbf{X}$  denote the centered log-ratio transformed (Aitchison, 1982) abundance matrix of  $p = 114$  taxa from  $n = 174$  observations. Let  $\mathcal{J} = \mathbf{I}_n - \frac{1}{n}\mathbf{1}\mathbf{1}^\top$ , where  $\mathbf{1}$  is the  $n \times 1$  vector of ones. The auxiliary row structure  $\mathbf{H}$  is obtained by  $\mathbf{H} = -\frac{1}{2}\mathcal{J}\Delta_{\mathbf{H}}\mathcal{J}$ , where  $\Delta_{\mathbf{H}}$  is the weighted UniFrac distance matrix between observations (Lozupone and Knight, 2005). This study design implies that the row structure of  $\mathbf{X}$  is inherent in  $\mathbf{H}$  from both the repeated measures and the UniFrac similarities among samples. The column structure  $\mathbf{Q}$  is a matrix of patristic similarities between taxa obtained from the phylogenetic tree. Letting  $\mathbf{d}_j$  denote the  $j$ -th eigenvector of  $\mathbf{Q}$ , we set

$$\boldsymbol{\beta}_0 = 2 \sum_{j=1}^{10} j^{-1/2} \mathbf{d}_j,$$

which resides in the space spanned by the top 10 eigenvectors of  $\mathbf{Q}$ . We further defined the true signal  $\boldsymbol{\beta}^*$  as a thresholded version of  $\boldsymbol{\beta}_0$ :  $\boldsymbol{\beta}^* = s(\boldsymbol{\beta}_0, 0.2)$ , where  $s(x, \tau)$  is the hard-thresholding operator; i.e.,  $s(x, \tau) = xI(|x| > \tau)$ , and the threshold  $\tau = 0.2$  was selected such that 55 entries of  $\boldsymbol{\beta}^*$  are exactly 0. The reason why we considered this thresholded parameter as our true parameter is two-folds. First,  $\boldsymbol{\beta}^*$  has both zero and nonzero entries, making it possible to evaluate the type-I error rate from testing the zero coefficients and the power from testing the non-zero coefficients. In comparison, all entries of  $\boldsymbol{\beta}_0$  are non-zero due to the structure of  $\mathbf{Q}$ . Second, while  $\boldsymbol{\beta}_0$  is completely informed by the top eigenvectors of  $\mathbf{Q}$ ,  $\boldsymbol{\beta}^*$  is only partially informed by  $\mathbf{Q}$ , which is more common in practice. Also, the derived theoretical results still hold when a small portion of the true parameter is not aligned with the top eigenvectors of  $\mathbf{Q}$  (see Assumptions (A2)).

Let  $\mathbf{H} = \sum_{j=1}^n \lambda_{j,H} \mathbf{d}_{j,H} \mathbf{d}_{j,H}^\top$  denote the eigen-decomposition of  $\mathbf{H}$ , where  $\lambda_{1,H} \geq \lambda_{2,H} \geq \dots \geq \lambda_{n,H} > 0$  are the eigenvalues, and  $\mathbf{d}_{1,H}, \dots, \mathbf{d}_{n,H}$  are the corresponding eigenvectors.

Defining

$$\Psi = \mathbf{H}^{-1} + \delta \mathbf{d}_{n,H} \mathbf{d}_{n,H}^\top,$$

we simulated the outcome  $\mathbf{y} = \mathbf{X}\boldsymbol{\beta}^* + \boldsymbol{\epsilon}$ , where  $\boldsymbol{\epsilon}$  was generated from a multivariate normal distribution with mean  $\mathbf{0}$  and covariance  $\Psi$ . In this case, one can check that Assumption (A1) approximately holds with

$$\|\mathbf{L}_\psi \mathbf{H} \mathbf{L}_\psi^\top - \mathbf{I}_n\| = \delta \lambda_{n,H},$$

where  $\Psi = \mathbf{L}_\psi^\top \mathbf{L}_\psi$ . Thus, smaller  $\delta$  indicates that  $\mathbf{H}$  better informs  $\Psi$ ; in particular,  $\delta = 0$  means that  $\mathbf{H}$  fully informs  $\Psi$ .

We consider three values of  $\delta$ : 0, 10 and 100 such that  $\|\mathbf{L}_\psi \mathbf{H} \mathbf{L}_\psi^\top - \mathbf{I}_n\|$  is 0, 0.005 and 0.05, respectively. The results are summarized in Fig. 4. When  $\delta = 0$  or 10; i.e.,  $\mathbf{H}$  is fully or partially informative of  $\Psi$ , all methods can (asymptotically) control the type-I error rate (Ridge has a little inflation). However, when  $\delta = 100$ , meaning that  $\mathbf{H}$  becomes less informative, GMDI-d has an inflated type-I error rate. Inspecting Fig. 4B shows that both GMDI-k and GMDI-d have considerably higher power than existing methods. Similar to Simulation I, compared to GMDI-d, GMDI-k shows more stringent type-I error rate control and lower power.

## 5 Analysis of Microbiome Data

In this section, we illustrate the proposed GMDR and GMDI by analyzing real microbiome data from Yatsunenکو et al. (2012). The data consists of the counts of  $p = 149$  genera sampled from  $n = 100$  individuals from the Amazonas of Venezuela, rural Malawi and US metropolitan areas. In the original study, marginal analyses identified a large number of age-associated bacterial genera shared in all three populations.

For our analysis, to make the measurements comparable between subjects, we applied the centered log-ratio (CLR) transformation to obtain the data matrix  $\mathbf{X}$ . The column

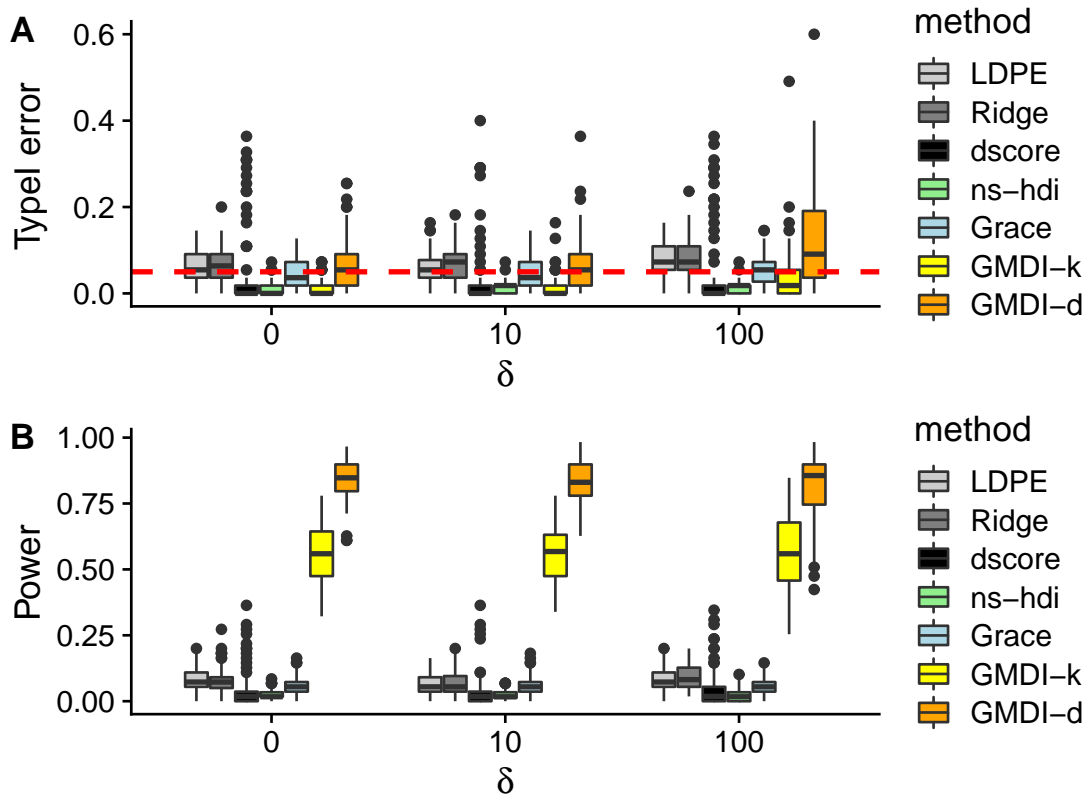


Figure 4: Boxplots of the type-I error (A) and power (B) over 500 replications for Simulation II with  $\delta = 0, 10$  and  $100$  : Both GMDI-d and GMDI-k can (asymptotically) control the type-I error, and have considerably higher power than other methods.

structure in  $\mathbf{X}$  is informed by a  $p \times p$  similarity kernel derived from the patristic distance between each pair of the tips of the phylogenetic tree, and the row structure is calculated from an  $n \times n$  sample similarity kernel based on the KEGG Enzyme Commissions (EC) number in each sample; these EC data represent counts of 432 classes of enzymes observed in the bacteria from the same 100 individuals. We also applied the CLR transformation to rows of the EC data and centered its columns to have mean 0. The resulting matrix is denoted by  $\mathbf{Z}$ , and the row structure is then given by  $n\{\mathbf{Z}\mathbf{Z}^\top\}^{-1}$ . For ease of presen-

tation, we denote the row and column structure respectively by  $\mathbf{H}^M$  and  $\mathbf{Q}^M$ . Similar to Yatsunenکو et al. (2012), we are interested in identifying age-associated bacterial genera. As the distribution of age is highly skewed (around 70% of the samples are below 3 years of age), we took the logarithm of age as our outcome, denoted by  $\mathbf{y}$ . We first examined the marginal association between each bacterial genus and age by regressing  $\mathbf{y}$  on each column of  $\mathbf{X}$ . Fig. 5 is a volcano plot of the log 10-transformed  $p$ -values versus the estimated regression coefficients. Blue dots represent bacteria that are not statistically significant ( $p > 0.05$ ); purple dots represent bacteria that are significant ( $p \leq 0.05$ ) but not significant after controlling the false discovery rate (FDR) at 0.1 using the Benjamini–Yekutieli procedure (Benjamini and Yekutieli, 2001); red dots represent bacteria that are still significant after controlling the FDR at 0.1. It can be seen that the majority of bacteria (105 out of 149) are marginally significant after controlling for FDR at 0.1. This is consistent with the results of the marginal Spearman correlations between each bacterial genus and age reported in Yatsunenکو et al. (2012).

However, since bacteria do not live independently, it is more interesting to examine the conditional association between each bacterial genus and age. Two possible explanations for the large number of marginal associations shown in Fig. 5 may be that (i) a large number of bacterial genera are conditionally associated with age; (ii) these bacteria are highly correlated, but only a few of these are conditionally associated with age. In both situations, existing high-dimensional inferential procedures may fail because either the regression coefficients are not sparse, or the restricted eigenvalue-type condition is no longer satisfied due to the highly correlated variables. However, our GMDI may still work in these situations because of its ability to address these two issues by incorporating informative structures. Thus, we first constructed multiple GMDR/KPR estimators and evaluated the prediction performance of these estimators. The GMDI was then applied based on the estimator with the best prediction performance to detect conditional associations between bacterial genera and age.

More specifically, to examine the informativeness of  $\mathbf{H}^M$  and  $\mathbf{Q}^M$ , we constructed the

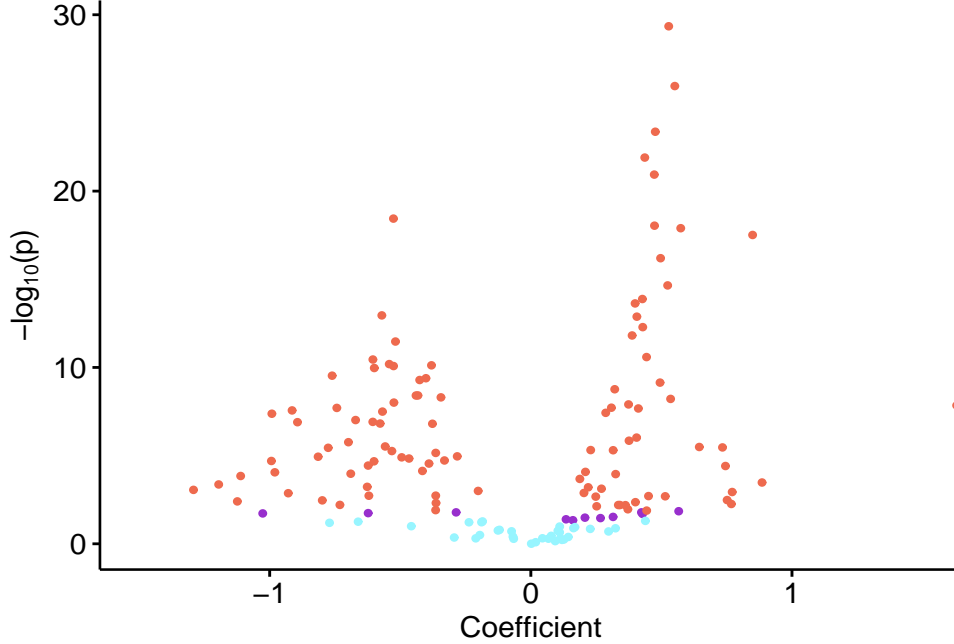


Figure 5: Marginal analysis: behaviors of the log10-transformed  $p$ -values versus the estimated regression coefficients. Blue dots represent bacteria that are not statistically significant ( $p > 0.05$ ); purple dots represent bacteria that are significant ( $p \leq 0.05$ ) but not significant after controlling the FDR at 0.1; red dots represent bacteria that are still significant after controlling the FDR at 0.1.

KPR and GMDR estimators based on three choices of  $\mathbf{H}$  and  $\mathbf{Q}$ : (i)  $\mathbf{H} = \mathbf{I}_n$ ;  $\mathbf{Q} = \mathbf{Q}^M$ , (ii)  $\mathbf{H} = \mathbf{H}^M$ ;  $\mathbf{Q} = \mathbf{I}_p$  and (iii)  $\mathbf{H} = \mathbf{H}^M$ ;  $\mathbf{Q} = \mathbf{Q}^M$ . We denote the KPR (GMDR) estimator corresponding to the first, second and third choice by KPR1 (GMDR1), KPR2 (GMDR2) and KPR3 (GMDR3), respectively. We examined the prediction performance of these estimators along with two classical methods: (i) the lasso estimator (Tibshirani, 1996) and (ii) the Ridge estimator (Hoerl and Kennard, 1970). Mean squared errors (MSE) for all the methods based on leave-one-out cross validation are displayed in Table 1. Both KPR1 and GMDR1 yield more accurate prediction results than Ridge, indicating the informativeness of the phylogenetic structure in terms of prediction. Similarly, KPR2 and GMDR2

Table 1: Mean squared errors (MSEs) for different methods.

Method	lasso	Ridge	KPR1	GMDR1	KPR2	GMDR2	KPR3	GMDR3
MSE	0.71	1.13	0.61	0.57	0.78	0.76	0.56	0.52

have higher prediction accuracy than Ridge, indicating that the individuals may exhibit non-trivial correlations, which the EC data can reliably characterize. Consequently, by incorporating information from both the phylogenetic structure and the EC data, KPR3 and GMDR3 further improve the prediction accuracy, and GMDR3 yields the highest prediction accuracy. Note that the Ridge estimator and all KPR and GMDR estimators belong to  $\mathcal{B}_{\text{GMD}}$  (see (5)), so these estimators are all based on GMD components with respect to different two-way structures. Hence, the superior prediction performance of KPR3 and GMDR3 demonstrates the predictive value of the GMD components that incorporate information from  $\mathbf{H}^M$  and  $\mathbf{Q}^M$ . It is also worth noting that every GMDR estimator yields higher prediction accuracy than its corresponding KPR estimator; this may be because of the proposed GCV procedure that guarantees the prediction accuracy of GMDR. As a reference, the prediction accuracy of lasso is higher than KPR2 and GMDR2 but lower than other GMDR and KPR estimators.

We next applied GMDI based on GMDR3 to detect conditional associations between bacterial genera and age, compared to the Grace test (Zhao and Shojaie, 2016), Ridge test (Bühlmann, 2013) and LDPE (Zhang and Zhang, 2014). The Grace test was implemented using  $\mathbf{L} = \mathbf{Q}^M$ . Genera found significantly associated with age when controlling for FDR at 0.1 are reported in Table 2. While the Ridge test results in no genera associated with age when controlling for FDR at 0.1, the Grace test and LDPE are able to detect 2 and 3 genera, respectively. Notably, by incorporating the auxiliary information, GMDI detects considerably more genera. Moreover, the genera detected by LDPE and the Grace test are also detected by GMDI. One particular bacterial genus, *Lactobacillus*, identified by GMDI but not by LDPE or the Grace test, is highlighted in Yatsunenکو et al. (2012) as one of the dominant baby gut microbiota. This may indicate the informativeness of  $\mathbf{H}^M$  and  $\mathbf{Q}^M$ .

Table 2: Genera found to be associated with age when controlling for FDR at 0.1 using the Ridge test, LDPE, the Grace test, and GMDI.

	Genus	Total
Ridge	(none)	0
LDPE	<i>Atopobium, Campylobacter, Peptoniphilus</i>	3
Grace	<i>Atopobium, Campylobacter</i>	2
GMDI	<i>Acidaminococcus, Aggregatibacter, Akkermansia, Alkalimonas, Anaerofustis, Anaerostipes, Arthrobacter, Atopobium, Bilophila, Brochothrix, Bulleidia, Butyrivibrio, Caloramator, Campylobacter, Citrobacter, Coprobacillus, Desulfotobacterium, Enterobacter, Epulopiscium, Faeklamia, Lachnobacterium, Lactobacillus, Leclercia, Megasphaera, Methylophaga, Mitsuokella, Peptococcus, Peptoniphilus, Roseburia, Ruminococcus, Rummeliibacillus, Slackia, Sphingobacterium, Sphingomonas, Streptococcus, Thiomonas, Xenorhabdus</i>	37

for identifying age-associated bacterial genera.

## 6 Discussions

This article studies high-dimensional linear regression with two-way structured data in terms of estimation and inference. For estimation, we develop GMDR that accounts for arbitrary pre-specified two-way structures. For inference of individual regression coefficients, we propose GMDI, a general high-dimensional inferential framework for a large family of estimators that include the GMDR estimator. Compared to existing high-dimensional inferential tools, GMDI does not require the true regression coefficients to be sparse, allows dependent and heteroscedastic samples, and provides more flexibility for users to specify relevant auxiliary row and column structures.

The proposed GMDR and GMDI also provide an approach for integrative analysis of multi-view data; i.e., data collected from multiple sources on the same subjects (Chen et al., 2010; Guo, 2013; Wang et al., 2013; Li and Li, 2019). As demonstrated in Section 5, the

row structure can be obtained from another data set that collects different features on the same set of samples. Analogously, when there are additional studies addressing the same scientific question, in other words, measuring the same set of variables, one can obtain the column structure from these studies in a similar way.

While the proposed method is motivated and illustrated using microbiome data, our method is generally applicable to arbitrary two-way structured data, such as gene expression data and neuroimaging data. It is often possible to obtain informative auxiliary row and/or column structures in these areas. For the analysis of gene expression data, one can obtain graph-structured prior information on the genes from, for example, Kyoto Encyclopedia of Genes and Genomes (KEGG, Kanehisa (2000)) or NCI Pathway Interaction Database (Schaefer et al., 2009). For the analysis of neuroimaging data, these structures are often defined as smoothing matrices relevant to the spatial/temporal structure of the images.

As a robust alternative to fully trusting the auxiliary structures or completely ignoring them, we can combine the observed structures and the identity matrix  $\mathbf{I}$  through some weight  $\pi \in [0, 1]$ . Take the column structure  $\mathbf{Q}$  as an example. For a given  $\pi \in [0, 1]$ , we can consider  $\mathbf{Q}(\pi) = \pi\mathbf{Q} + (1-\pi)\mathbf{I}$ . Large value of  $\pi$  favors the information in  $\mathbf{Q}$ , while small value of  $\pi$  protects the analysis being affected by bad choices of  $\mathbf{Q}$ . This idea, which was also considered in Zhao and Shojaie (2016), can be straightforwardly extended to multiple auxiliary structures,  $\mathbf{Q}_1, \dots, \mathbf{Q}_L$ , for some  $L \geq 2$ . Let  $\boldsymbol{\pi} = (\pi_1, \dots, \pi_L)^\top$  with  $\pi_l \geq 0$  for  $l = 1, \dots, L$  and  $\sum_{l=1}^L \pi_l \leq 1$ , and one can consider  $\mathbf{Q}(\boldsymbol{\pi}) = \sum_{l=1}^L \pi_l \mathbf{Q}_l + \left(1 - \sum_{l=1}^L \pi_l\right) \mathbf{I}$ . In practice, one can find the  $\boldsymbol{\pi}$  that yields the best prediction accuracy. We leave the investigation of this data adaptive procedure to future research.



# Appendix

## (A1) Derivations of Eq. (6)

We only focus on the high-dimensional case where  $K = n < p$ , noting that similar derivations can be straightforwardly applied to the case where  $K > p$ . It follows from the definition of  $\hat{\boldsymbol{\beta}}_{\text{KPR}}(\eta)$  that

$$\begin{aligned}\hat{\boldsymbol{\beta}}_{\text{KPR}}(\eta) &= (\mathbf{X}^\top \mathbf{H} \mathbf{X} + \eta \mathbf{Q}^{-1})^{-1} \mathbf{X}^\top \mathbf{H} \mathbf{y} \\ &= \mathbf{Q} (\mathbf{X}^\top \mathbf{H} \mathbf{X} \mathbf{Q} + \eta \mathbf{I}_p)^{-1} \mathbf{X}^\top \mathbf{H} \mathbf{y} \\ &= \mathbf{Q} \mathbf{X}^\top \mathbf{H} (\mathbf{X} \mathbf{Q} \mathbf{X}^\top \mathbf{H} + \eta \mathbf{I}_n)^{-1} \mathbf{y}.\end{aligned}$$

Since the GMD of  $\mathbf{X}$  yields  $\mathbf{X} = \mathbf{U} \mathbf{S} \mathbf{V}^\top$ , we get

$$\begin{aligned}\hat{\boldsymbol{\beta}}_{\text{KPR}}(\eta) &= \mathbf{Q} \mathbf{V} \mathbf{S} \mathbf{U}^\top \mathbf{H} (\mathbf{U} (\mathbf{S}^2 + \eta \mathbf{I}_n) \mathbf{U}^\top \mathbf{H})^{-1} \mathbf{y} \\ &= \mathbf{Q} \mathbf{V} \mathbf{S}^{-1} \mathbf{S}^2 (\mathbf{S}^2 + \eta \mathbf{I}_n)^{-1} \mathbf{U}^\top \mathbf{H} \mathbf{y}.\end{aligned}\tag{19}$$

The last equality in (19) comes from the fact that  $\mathbf{U}$  is a  $n \times n$  invertible matrix and  $\mathbf{U}^\top \mathbf{H} \mathbf{U} = \mathbf{I}_n$ . Denoting  $\mathbf{W}_\eta = \mathbf{S}^2 (\mathbf{S}^2 + \eta \mathbf{I}_n)^{-1}$ , we can write

$$\hat{\boldsymbol{\beta}}_{\text{KPR}}(\eta) = \mathbf{Q} \mathbf{V} \mathbf{S}^{-1} \mathbf{W}_\eta \mathbf{U}^\top \mathbf{H} \mathbf{y}.\tag{20}$$

## (A2) Proof of Propositions 3.1 and 3.2

We first recall the definition of  $\hat{\beta}_j^w(h_j)$  in (9) as follows.

$$\hat{\beta}_j^w(h_j) = \beta_j^w - \hat{B}_j(h_j).$$

Plugging in the definition of  $\beta_j^w$  and  $\widehat{B}_j(h_j)$ , we get

$$\begin{aligned}
\widehat{\beta}_j^w(h_j) &= \sum_{m \neq j} \xi_{jm}^w \beta_m^* + \xi_{jj}^w \beta_j^* - \sum_{m \neq j} \xi_{jm}^w \beta_m^{init} - h_j (\xi_{jj}^w - 1) \beta_j^{init} + Z_j^w \\
&= ((1 - h_j) \xi_{jj}^w + h_j) \beta_j^* + \sum_{m \neq j} \xi_{jm}^w (\beta_m^* - \beta_m^{init}) + \\
&\quad h_j (\xi_{jj}^w - 1) (\beta_j^* - \beta_j^{init}) + Z_j^w,
\end{aligned} \tag{21}$$

where  $Z_j^w = \sum_{i=1}^n a_{ji} \tilde{\epsilon}_i$ . To prove the asymptotic normality of  $Z_j^w$ , we first check the Lindeberg's condition; that is,

$$\lim_{n \rightarrow \infty} \frac{1}{s_{n,j}^2} \sum_{i=1}^n \mathbb{E} [a_{ji}^2 \tilde{\epsilon}_i^2 \times I \{|a_{ji} \tilde{\epsilon}_i| > t s_{n,j}\}] = 0, \text{ for all } t > 0,$$

where  $s_{n,j}^2 = \sum_{i=1}^n a_{ji}^2$ . Let  $\varepsilon$  be a random variable distributed like every  $\tilde{\epsilon}_i$ . Then,

$$\begin{aligned}
\frac{1}{s_{n,j}^2} \sum_{i=1}^n \mathbb{E} [a_{ji}^2 \tilde{\epsilon}_i^2 \times I \{|a_{ji} \tilde{\epsilon}_i| > t s_{n,j}\}] &= \frac{1}{s_{n,j}^2} \sum_{i=1}^n \{a_{ji}^2 \mathbb{E} [\varepsilon^2 \times I \{|\varepsilon| > t s_{n,j} |a_{ji}|^{-1}\}]\} \\
&\leq \frac{1}{s_{n,j}^2} \left( \sum_{i=1}^n a_{ji}^2 \right) \mathbb{E} \left[ \varepsilon^2 \times I \left\{ |\varepsilon| > t s_{n,j} \left\{ \max_{i=1, \dots, n} |a_{ji}| \right\}^{-1} \right\} \right] \\
&= \mathbb{E} \left[ \varepsilon^2 \times I \left\{ |\varepsilon| > \frac{t \sqrt{\sum_{i=1}^n a_{ji}^2}}{\max_{i=1, \dots, n} |a_{ji}|} \right\} \right].
\end{aligned}$$

Since

$$\lim_{n \rightarrow \infty} \frac{\max_{i=1, \dots, n} |a_{ji}|}{\sqrt{\sum_{i=1}^n a_{ji}^2}} = 0,$$

by using the dominated convergence theorem, we get

$$\lim_{n \rightarrow \infty} \frac{1}{s_{n,j}^2} \sum_{i=1}^n \mathbb{E} [a_{ji}^2 \tilde{\epsilon}_i^2 \times I \{|a_{ji} \tilde{\epsilon}_i| > t s_{n,j}\}] = 0 \text{ for all } t > 0.$$

Next, using the Lindeberg central limit theorem, we get  $s_{n,j}^{-1}Z_j^w \xrightarrow{d} N(0,1)$  as  $n \rightarrow \infty$ . Lastly, we find the explicit form of  $s_{n,j}$  by noting that

$$s_{n,j}^2 = \sum_{i=1}^n a_{ji}^2 = (\mathbf{Q}\mathbf{V}\mathbf{W}\mathbf{S}^{-1}\mathbf{U}^\top\mathbf{H}\mathbf{L}_\psi^\top (\mathbf{Q}\mathbf{V}\mathbf{W}\mathbf{S}^{-1}\mathbf{U}^\top\mathbf{H}\mathbf{L}_\psi^\top)^\top)_{(j,j)} = \Omega_{jj}^w,$$

which completes the proof of Proposition 3.1.

Next we prove Proposition 3.2. Recall that  $R_{jj}^w = \{\mathbf{Q}\mathbf{V}\mathbf{W}^2\mathbf{S}^{-2}\mathbf{V}^\top\mathbf{Q}\}_{(j,j)}$ . Then, we can write

$$\Omega_{jj}^w = R_{jj}^w + \mathbf{e}_j^\top \mathbf{Q}\mathbf{V}\mathbf{W}\mathbf{S}^{-1}\mathbf{U}^\top\mathbf{H}^{1/2}(\mathbf{H}^{1/2}\mathbf{L}_\psi^\top\mathbf{L}_\psi\mathbf{H}^{1/2} - \mathbf{I}_n)\mathbf{H}^{1/2}\mathbf{U}\mathbf{S}^{-1}\mathbf{W}\mathbf{V}^\top\mathbf{Q}\mathbf{e}_j,$$

where  $\mathbf{e}_j \in \mathbb{R}^n$  is the vector with one in its  $j$ -th entry and zero elsewhere. By Assumption (A1), we know that  $\|\mathbf{H}^{1/2}\mathbf{L}_\psi^\top\mathbf{L}_\psi\mathbf{H}^{1/2} - \mathbf{I}_n\|_2 = \|\mathbf{L}_\psi\mathbf{H}\mathbf{L}_\psi^\top - \mathbf{I}_n\|_2 = o(1)$  as  $n \rightarrow \infty$ . Thus, we have

$$\mathbf{e}_j^\top \mathbf{Q}\mathbf{V}\mathbf{W}\mathbf{S}^{-1}\mathbf{U}^\top\mathbf{H}^{1/2}(\mathbf{H}^{1/2}\mathbf{L}_\psi^\top\mathbf{L}_\psi\mathbf{H}^{1/2} - \mathbf{I}_n)\mathbf{H}^{1/2}\mathbf{U}\mathbf{S}^{-1}\mathbf{W}\mathbf{V}^\top\mathbf{Q}\mathbf{e}_j = o(R_{jj}^w).$$

This further leads to

$$\frac{\Omega_{jj}^w}{R_{jj}^w} = 1 + o(1), \text{ as } n \rightarrow \infty.$$

Since  $Z_j^w/\sqrt{\Omega_{jj}^w} \xrightarrow{d} N(0,1)$ , we have

$$\frac{Z_j^w}{\sqrt{R_{jj}^w}} = \frac{Z_j^w}{\sqrt{\Omega_{jj}^w}} \times \sqrt{\frac{\Omega_{jj}^w}{R_{jj}^w}} \xrightarrow{d} N(0,1) \text{ as } n \rightarrow \infty.$$

This completes the proof of Proposition 3.2.

### (A3) Proof of Theorem 3.1

Recall that  $\check{\mathbf{X}} = \mathbf{H}^{1/2}\mathbf{X}\mathbf{D}\mathbf{\Delta}^{1/2}$  and  $\tilde{\boldsymbol{\beta}}^* = \mathbf{D}^\top\boldsymbol{\beta}^*$ . The next lemma characterizes  $\|\tilde{\boldsymbol{\beta}}(\lambda) - \tilde{\boldsymbol{\beta}}^*\|_1$ , where  $\tilde{\boldsymbol{\beta}}(\lambda)$  is given in (12).

**Lemma 6.1.** *Suppose that  $\|\mathbf{Q}\|_2 = 1$  and each column of  $\mathbf{X}$  has been scaled so that  $\|\mathbf{X}\mathbf{d}_j\|_{\mathbf{H}}^2 = n$  for  $j = 1, \dots, p$ , where  $\mathbf{d}_j$  is the  $j$ -th eigenvector of  $\mathbf{Q}$ . For any  $c_0 > 0$ , if*

$$\lambda = 2\sqrt{2c^*n \log p(1 + c_0)\|\mathbf{L}_\psi^\top \mathbf{H} \mathbf{L}_\psi\|_2},$$

*then under Assumptions (A1)–(A3), we have*

$$\left\| \tilde{\boldsymbol{\beta}}(\lambda) - \tilde{\boldsymbol{\beta}}^* \right\|_1 = O_p\left(s_0\sqrt{n^{-1} \log p}\right) \quad \text{as } n \rightarrow \infty.$$

*Lemma 6.1.* We first define some additional notations. For any index set  $A \subset \{1, \dots, p\}$ , let  $\check{\mathbf{X}}_A$  denote the submatrix of  $\check{\mathbf{X}}$  with columns indexed by  $A$ , and let  $\mathbf{P}_A$  denote the projection matrix onto the column space of  $\check{\mathbf{X}}_A$ . Define

$$\chi_m^* = \max_{|A|=m, \mathbf{s} \in \{\pm 1\}^m} \left| \frac{\boldsymbol{\varepsilon}' \check{\mathbf{X}}_A (\check{\mathbf{X}}_A' \check{\mathbf{X}}_A)^{-1} \mathbf{s} \lambda - (\mathbf{I} - \mathbf{P}_A) \check{\mathbf{X}} \boldsymbol{\Delta}^{-1/2} \tilde{\boldsymbol{\beta}}^*}{\left\| \check{\mathbf{X}}_A (\check{\mathbf{X}}_A' \check{\mathbf{X}}_A)^{-1} \mathbf{s} \lambda - (\mathbf{I} - \mathbf{P}_A) \check{\mathbf{X}} \boldsymbol{\Delta}^{-1/2} \tilde{\boldsymbol{\beta}}^* \right\|_2} \right|,$$

where  $\boldsymbol{\varepsilon} = \mathbf{H}^{1/2} \mathbf{L}_\psi \boldsymbol{\epsilon}$ , and  $\lambda > 0$  is the tuning parameter. For all  $m_0 \geq 0$ , define the following Borel set

$$\Omega_{m_0} \equiv \{\chi_m^* \leq t_m \quad \forall m \geq m_0\},$$

where

$$t_m = \sqrt{2 \log p(m \vee 1)(1 + c_0)\|\mathbf{L}_\psi^\top \mathbf{H} \mathbf{L}_\psi\|_2}$$

for some constant  $c_0 > 0$ . Let

$$r_1 \equiv \left(\frac{c^* \eta_1 n}{s_0 \lambda}\right)^{1/2}, \quad r_2 \equiv \left(\frac{c^* \eta_1^2 n}{s_0 \lambda^2}\right)^{1/2} \quad \text{and} \quad C \equiv \frac{c^*}{c_*}.$$

It can be checked that with the  $\eta_1$  specified in Assumption (A2) and the  $\lambda$  specified in Lemma 6.1,  $r_1$  and  $r_2$  are both  $O(1)$  quantities. Let  $M_1^* = 2 + 4r_1^2 + 4\sqrt{C}r_2 + 4C$ ,  $\tilde{S}_0 = \{j : \tilde{\beta}_j(\lambda) \neq 0\}$  and  $S_1 = \tilde{S}_0 \cup S_0$ . We follow the proof in Zhang et al. (2008), and summarize

the following three major steps.

1. According to the proof of Theorem 1 in Zhang et al. (2008) (see Equation (5.26) in Zhang et al. (2008) and its derivations), we have  $|S_1| \leq M_1^* s_0$  while conditioning on the event  $\Omega_{s_0}$ .

2. In the second step, we show that the event  $\Omega_{s_0}$  happens with high probability. In Zhang et al. (2008), this is proved for the setting where  $\boldsymbol{\varepsilon} \sim N(0, \sigma^2 \mathbf{I}_n)$ . However, in our case,  $\boldsymbol{\varepsilon}$  is not necessarily Gaussian, and its covariance matrix,  $\mathbf{H}^{1/2} \mathbf{L}_\psi^\top \mathbf{L}_\psi \mathbf{H}^{1/2}$ , is not necessarily equal to  $\mathbf{I}_n$  (up to a constant). To prove this, we first notice that for all  $s_0$ ,

$$\mathbb{P}(\Omega_{s_0}^c) \leq \mathbb{P}(\Omega_0^c) \leq \sum_{m=0}^{\infty} 2^{m \vee 1} \binom{p}{m} p_m, \quad (22)$$

where

$$p_m = \mathbb{P} \left( \left| \boldsymbol{\varepsilon}' \frac{\check{\mathbf{X}}_A (\check{\mathbf{X}}_A' \check{\mathbf{X}}_A)^{-1} \mathbf{s} \lambda - (\mathbf{I} - \mathbf{P}_A) \check{\mathbf{X}} \boldsymbol{\Delta}^{-1/2} \tilde{\boldsymbol{\beta}}^*}{\left\| \check{\mathbf{X}}_A (\check{\mathbf{X}}_A' \check{\mathbf{X}}_A)^{-1} \mathbf{s} \lambda - (\mathbf{I} - \mathbf{P}_A) \check{\mathbf{X}} \boldsymbol{\Delta}^{-1/2} \tilde{\boldsymbol{\beta}}^* \right\|_2} \right| \geq t_m \right)$$

with  $|A| = m$  and some  $\mathbf{s} \in \{\pm 1\}^m$ . Next we find an upper bound for  $p_m$ . Since  $\boldsymbol{\varepsilon} = \mathbf{H}^{1/2} \mathbf{L}_\psi \boldsymbol{\epsilon}$ , where  $\boldsymbol{\epsilon}$  has *i.i.d.* sub-Gaussian entries with mean 0 and variance 1, using the Hoeffding's inequality (Wainwright, 2019), we get

$$p_m \leq 2 \exp\left\{-\frac{t_m^2}{\|\mathbf{L}_\psi \mathbf{H} \mathbf{L}_\psi\|_2}\right\} = 2 \exp(-(m \vee 1)(1 + c_0) \log p). \quad (23)$$

Combining (22) and (23), we have

$$\begin{aligned}
\mathbb{P}(\Omega_{s_0}^c) &\leq \sum_{m=0}^{\infty} 2^{(m \vee 1)+1} \binom{p}{m} (p^{-(1+c_0)})^{m \vee 1} \\
&\leq \frac{4}{p^{1+c_0}} + 2 \sum_{m=1}^{\infty} 2^m \binom{p}{m} p^{-m(1+c_0)} \\
&= \frac{4}{p^{1+c_0}} + 2 \left( (1 + 2p^{-(1+c_0)})^p - 1 \right) \\
&\leq \frac{4}{p^{1+c_0}} + 2 \left( \exp(2p^{-c_0}) - 1 \right); \tag{24}
\end{aligned}$$

here, we use the binomial theorem and the fact that  $\lim_{x \rightarrow 0} (1+x)^{1/x} = e$ . Therefore, we have  $\mathbb{P}(\Omega_{s_0}) = 1 - \mathbb{P}(\Omega_{s_0}^c) \rightarrow 1$  as  $p \rightarrow \infty$ .

3. We use the techniques in the proof of Theorem 3 in Zhang et al. (2008) to bound  $\|\tilde{\beta}(\lambda) - \tilde{\beta}^*\|_1$  with the pre-specified  $\eta_1$  and  $\lambda$ . Recall that on the event  $\Omega_{s_0}$ , we have  $|S_1| \leq M_1^* s_0$ . Let  $\check{\mathbf{X}}_1$  and  $\check{\mathbf{X}}_2$ , respectively, denote the submatrix of  $\check{\mathbf{X}}$  with columns indexed by  $S_1$  and  $S_1^c$ . Similarly, let  $\tilde{\beta}_1^*$  and  $\tilde{\beta}_2^*$ , respectively, denote the subvector of  $\tilde{\beta}^*$  with entries indexed by  $S_1$  and  $S_1^c$ ;  $\tilde{\beta}_1(\lambda)$  and  $\tilde{\beta}_2(\lambda)$ , respectively, denote the subvector of  $\tilde{\beta}(\lambda)$  with entries indexed by  $S_1$  and  $S_1^c$ ;  $\Delta_1$  and  $\Delta_2$ , respectively, denote the submatrix of  $\Delta$  with both rows and columns indexed by  $S_1$  and  $S_1^c$ . Since  $q^* \geq M_1^* s_0 + 1$ , by Assumption (A3), the vector  $\mathbf{v}_1 = \check{\mathbf{X}}_1 \Delta_1^{-1/2} (\tilde{\beta}_1(\lambda) - \tilde{\beta}_1^*)$  satisfies

$$\|\mathbf{v}_1\|_2^2 \geq c_* n \left\| \Delta_1^{-1/2} (\tilde{\beta}_1(\lambda) - \tilde{\beta}_1^*) \right\|_2^2. \tag{25}$$

Denoting by  $\mathbf{P}_1$  the projection matrix onto the column space of  $\check{\mathbf{X}}_1$ , we have

$$\begin{aligned}
\|\mathbf{v}_1\|_2 &\leq \|\mathbf{v}_1 + \mathbf{P}_1(\tilde{\mathbf{y}} - \check{\mathbf{X}}_1\Delta_1^{-1/2}\tilde{\boldsymbol{\beta}}_1(\lambda))\|_2 + \|\mathbf{P}_1(\tilde{\mathbf{y}} - \check{\mathbf{X}}_1\Delta_1^{-1/2}\tilde{\boldsymbol{\beta}}_1(\lambda))\|_2 \\
&\leq \|\mathbf{P}_1\check{\mathbf{X}}_2\Delta_2^{-1/2}\tilde{\boldsymbol{\beta}}_2^* + \mathbf{P}_1\mathbf{H}^{1/2}\mathbf{L}_\psi\boldsymbol{\epsilon}\|_2 + \|\mathbf{P}_1(\tilde{\mathbf{y}} - \check{\mathbf{X}}_1\Delta_1^{-1/2}\tilde{\boldsymbol{\beta}}_1(\lambda))\|_2 \\
&\leq \|\check{\mathbf{X}}_2\Delta_2^{-1/2}\tilde{\boldsymbol{\beta}}_2^*\|_2 + \|\mathbf{P}_1\mathbf{H}^{1/2}\mathbf{L}_\psi\boldsymbol{\epsilon}\|_2 + n^{-1/2}\|\Sigma_{11}^{-1/2}\mathbf{g}_1\|_2,
\end{aligned} \tag{26}$$

where  $\Sigma_{11} \equiv n^{-1}\check{\mathbf{X}}_1^\top\check{\mathbf{X}}_1$ ,  $\tilde{\mathbf{y}} = \mathbf{H}^{1/2}\mathbf{y}$  and  $\mathbf{g}_1 = \check{\mathbf{X}}_1^\top(\tilde{\mathbf{y}} - \check{\mathbf{X}}_1\Delta_1^{-1/2}\tilde{\boldsymbol{\beta}}_1(\lambda))$ . Note that the KKT conditions of (12) yield that  $\|\mathbf{g}_1\|_\infty \leq \lambda$ . Then, by Assumption (A3), we have

$$\|\Sigma_{11}^{-1/2}\mathbf{g}_1\|_2 \leq c_*^{-1/2}\|\mathbf{g}_1\|_\infty\sqrt{|S_1|} \leq \lambda(M_1^*s_0/c_*)^{1/2}.$$

Also, since  $S_1^c \subset S_0^c$ ,  $\|\mathbf{X}\mathbf{d}_j\|_{\mathbf{H}}^2 = n$ , and  $\|\mathbf{Q}\|_2 = 1$ , we have  $\|\check{\mathbf{X}}_2\Delta_2^{-1/2}\tilde{\boldsymbol{\beta}}_2^*\|_2 \leq \sqrt{n}\eta_1$ . We next find an upper bound for  $\|\mathbf{P}_1\mathbf{H}^{1/2}\mathbf{L}_\psi\boldsymbol{\epsilon}\|_2$ . Using the Hanson-Wright inequality (Theorem 2.1 in Rudelson et al. (2013)), we have

$$\mathbb{P}\left(\|\mathbf{P}_1\mathbf{H}^{1/2}\mathbf{L}_\psi\boldsymbol{\epsilon}\|_2 \geq \|\mathbf{P}_1\mathbf{H}^{1/2}\mathbf{L}_\psi\|_F + t\right) \leq \exp\left\{-\frac{ct^2}{\|\mathbf{P}_1\mathbf{H}^{1/2}\mathbf{L}_\psi\|_2^2}\right\}, \tag{27}$$

for some constant  $c$ . By properties of matrix norms, we have

$$\|\mathbf{P}_1\mathbf{H}^{1/2}\mathbf{L}_\psi\|_2^2 \leq \|\mathbf{L}_\psi^\top\mathbf{H}\mathbf{L}_\psi\|_2; \|\mathbf{P}_1\mathbf{H}^{1/2}\mathbf{L}_\psi\|_F^2 \leq \|\mathbf{L}_\psi^\top\mathbf{H}\mathbf{L}_\psi\|_2|S_1|;$$

here, we use the facts that  $\|\mathbf{P}_1\|_2 = 1$  and  $\|\mathbf{P}_1\|_F = |S_1|$ . Thus,

$$\mathbb{P}\left(\|\mathbf{P}_1\mathbf{H}^{1/2}\mathbf{L}_\psi\boldsymbol{\epsilon}\|_2 \geq \sqrt{\|\mathbf{L}_\psi^\top\mathbf{H}\mathbf{L}_\psi\|_2|S_1|} + t\right) \leq \exp\left\{-\frac{ct^2}{\|\mathbf{L}_\psi^\top\mathbf{H}\mathbf{L}_\psi\|_2}\right\}.$$

Letting  $t^2 = \|\mathbf{L}_\psi^\top\mathbf{H}\mathbf{L}_\psi\|_2|S_1|\log p$ , there exists a Borel set  $\tilde{\Omega}$  with  $\mathbb{P}(\tilde{\Omega}) \rightarrow 1$  as  $p \rightarrow \infty$ ,

such that on this set

$$\|\mathbf{P}_1 \mathbf{H}^{1/2} \mathbf{L}_\psi \boldsymbol{\epsilon}\|_2 \leq \sqrt{\|\mathbf{L}_\psi^\top \mathbf{H} \mathbf{L}_\psi\|_2 |S_1|} \left(1 + \sqrt{\log p}\right). \quad (28)$$

Therefore, on the event  $\Omega_{s_0} \cap \tilde{\Omega}$ , we have

$$\|\mathbf{P}_1 \mathbf{H}^{1/2} \mathbf{L}_\psi \boldsymbol{\epsilon}\|_2 \leq \sqrt{\|\mathbf{L}_\psi^\top \mathbf{H} \mathbf{L}_\psi\|_2 M_1^* s_0} \left(1 + \sqrt{\log p}\right).$$

Thus,

$$\begin{aligned} \left\| \boldsymbol{\Delta}_1^{-1/2} \left( \tilde{\boldsymbol{\beta}}_1(\lambda) - \tilde{\boldsymbol{\beta}}_1^* \right) \right\|_2 &\leq (c_* n)^{-1/2} \|\mathbf{v}_1\|_2 \\ &\leq c_*^{-1/2} \eta_1 + n^{-1/2} \sqrt{\|\mathbf{L}_\psi^\top \mathbf{H} \mathbf{L}_\psi\|_2 M_1^* s_0} \left(1 + \sqrt{\log p}\right) \\ &\quad + n^{-1/2} \lambda \left( \frac{M_1^* s_0}{nc_*} \right)^{1/2}. \end{aligned} \quad (29)$$

Since  $\lambda = 2\sqrt{2c_* n \log p (1 + c_0) \|\mathbf{L}_\psi^\top \mathbf{H} \mathbf{L}_\psi\|_2}$ ,  $\|\mathbf{L}_\psi^\top \mathbf{H} \mathbf{L}_\psi\|_2 = 1 + o(1)$ ,  $\eta_1 = O\left(\sqrt{n^{-1} s_0 \log p}\right)$  and  $M_1^* = O(1)$ , we have

$$\left\| \tilde{\boldsymbol{\beta}}_1(\lambda) - \tilde{\boldsymbol{\beta}}_1^* \right\|_2 \leq \left\| \boldsymbol{\Delta}_1^{1/2} \right\|_2 \left\| \boldsymbol{\Delta}_1^{-1/2} \left( \tilde{\boldsymbol{\beta}}_1(\lambda) - \tilde{\boldsymbol{\beta}}_1^* \right) \right\|_2 = O_p\left(\sqrt{n^{-1} s_0 \log p}\right).$$

Therefore,

$$\left\| \tilde{\boldsymbol{\beta}}_1(\lambda) - \tilde{\boldsymbol{\beta}}_1^* \right\|_1 \leq \sqrt{s_0} \left\| \tilde{\boldsymbol{\beta}}_1(\lambda) - \tilde{\boldsymbol{\beta}}_1^* \right\|_2 = O_p\left(s_0 \sqrt{n^{-1} \log p}\right).$$

Finally,

$$\left\| \tilde{\boldsymbol{\beta}}(\lambda) - \tilde{\boldsymbol{\beta}}^* \right\|_1 \leq \left\| \tilde{\boldsymbol{\beta}}_1(\lambda) - \tilde{\boldsymbol{\beta}}_1^* \right\|_1 + \eta_1 = O_p\left(s_0 \sqrt{n^{-1} \log p}\right).$$

This completes the proof.  $\square$

Now we use Lemma 6.1 to prove Theorem 3.1. First, note that since  $s_0 = o((n/\log p)^r)$



for some  $r \in (0, 1/2)$ , we have

$$\left\| \tilde{\boldsymbol{\beta}}^* - \tilde{\boldsymbol{\beta}}(\lambda) \right\|_1 = o_p \left\{ \left( \frac{\log p}{n} \right)^{1/2-r} \right\}. \quad (30)$$

Thus,

$$\begin{aligned} |\zeta_j(h_j)| &= \left| \sum_{m=1}^p \xi_{jm}^w (\beta_m^* - \beta_m^{init}) - ((1-h_j)\xi_{jj}^w + h_j) (\beta_j^* - \beta_j^{init}) \right| \\ &= \left| [(\mathbf{Q}\mathbf{V}\mathbf{W}\mathbf{V}^\top - (1-h_j)\boldsymbol{\Xi} - h_j\mathbf{I}_p) (\boldsymbol{\beta}^* - \boldsymbol{\beta}^{init})]_j \right| \\ &\leq \left\| [(\mathbf{Q}\mathbf{V}\mathbf{W}\mathbf{V}^\top - (1-h_j)\boldsymbol{\Xi} - h_j\mathbf{I}_p) \mathbf{D}]_{(j,\cdot)} \right\|_\infty \left\| \tilde{\boldsymbol{\beta}}^* - \tilde{\boldsymbol{\beta}}(\lambda) \right\|_1. \end{aligned} \quad (31)$$

Combining (30) and (31), it can be seen that

$$\lim_{n \rightarrow \infty} \Pr \left\{ |\zeta_j(h_j)| \leq \left\| [(\mathbf{Q}\mathbf{V}\mathbf{W}\mathbf{V}^\top - (1-h_j)\boldsymbol{\Xi} - h_j\mathbf{I}_p) \mathbf{D}]_{(j,\cdot)} \right\|_\infty \left( \frac{\log p}{n} \right)^{1/2-r} \right\} = 1.$$

Finally, (13) directly follows from Propositions 3.1 and 3.2.

## (A4) Proof of Theorem 3.2

We first note that  $P_j^w(h_j) \leq \alpha$  is equivalent to

$$\left| \hat{\beta}_j^w(h_j) \right| \geq \Psi_j(h_j) + q_{(1-\alpha/2)} \sqrt{R_{jj}^w}.$$

Since  $\left| \hat{\beta}_j^w(h_j) \right| = \left| ((1-h_j)\xi_{jj}^w + h_j) \beta_j^* + \zeta_j(h_j) + Z_j^w \right|$ , we have

$$\begin{aligned} &\Pr \left\{ \left| \hat{\beta}_j^w(h_j) \right| \geq \Psi_j(h_j) + q_{(1-\alpha/2)} \sqrt{R_{jj}^w} \right\} \geq \\ &\Pr \left\{ \left| ((1-h_j)\xi_{jj}^w + h_j) \beta_j^* \right| - |\zeta_j(h_j)| - |Z_j^w| \geq \Psi_j(h_j) + q_{(1-\alpha/2)} \sqrt{R_{jj}^w} \right\}. \end{aligned}$$

Hence, it suffices to show that as  $n \rightarrow \infty$ ,

$$\Pr \left\{ \left| \left( (1 - h_j) \xi_{jj}^w + h_j \right) \beta_j^* \right| - |\zeta_j(h_j)| - |Z_j^w| \geq \Psi_j(h_j) + q_{(1-\alpha/2)} \sqrt{R_{jj}^w} \right\} \geq \psi. \quad (32)$$

Since  $(R_{jj}^w)^{-1/2} Z_j^w \xrightarrow{d} N(0, 1)$  as  $n \rightarrow \infty$ , if

$$\frac{\left| \left( (1 - h_j) \xi_{jj}^w + h_j \right) \beta_j^* \right| - |\zeta_j(h_j)| - \Psi_j(h_j) - q_{(1-\alpha/2)} \sqrt{R_{jj}^w}}{\sqrt{R_{jj}^w}} \geq q_{(1-\psi/2)}, \quad (33)$$

then (32) holds. Since  $\lim_{n \rightarrow \infty} \Pr(|\zeta_j(h_j)| \leq \Psi_j(h_j)) = 1$  (Theorem 3.1), we know that as  $n \rightarrow \infty$ , (33) holds if

$$|\beta_j^*| \geq \left| (1 - h_j) \xi_{jj}^w + h_j \right|^{-1} \left( 2\Psi_j(h_j) + \left( q_{(1-\alpha/2)} + q_{(1-\psi/2)} \right) \sqrt{R_{jj}^w} \right);$$

this completes of proof of Theorem 3.2.

## References

- Aitchison, J. (1982). The statistical analysis of compositional data. *Journal of the Royal Statistical Society: Series B (Methodological)* 44(2), 139–160.
- Allen, G. I., L. Grose, and J. Taylor (2014). A generalized least-square matrix decomposition. *Journal of the American Statistical Association* 109(505), 145–159.
- Benjamini, Y. and D. Yekutieli (2001). The control of the false discovery rate in multiple testing under dependency. *The Annals of Statistics* 29(4), 1165–1188.
- Bühlmann, P. (2013). Statistical significance in high-dimensional linear models. *Bernoulli* 19(4), 1212–1242.
- Caporaso, J. G., J. Kuczynski, J. Stombaugh, K. Bittinger, F. D. Bushman, E. K. Costello,

- N. Fierer, A. G. Pena, J. K. Goodrich, J. I. Gordon, et al. (2010). Qiime allows analysis of high-throughput community sequencing data. *Nature methods* 7(5), 335–336.
- Chen, N., J. Zhu, and E. P. Xing (2010). Predictive subspace learning for multi-view data: a large margin approach. In *Advances in Neural Information Processing Systems 23*, pp. 361–369. Curran Associates, Inc.
- Cook, R. D. (2007). Fisher lecture: Dimension reduction in regression. *Statistical Science* 22(1), 1–26.
- Escoufier, Y. (1987). The duality diagram: a means for better practical applications. In *Develoments in Numerical Ecology*, pp. 139–156. Springer.
- Escoufier, Y. (2006). Operator related to a data matrix: a survey. In A. Rizzi and M. Vichi (Eds.), *Compstat 2006 - Proceedings in Computational Statistics*, Heidelberg, pp. 285–297. Physica-Verlag HD.
- Friedman, J., T. Hastie, R. Tibshirani, et al. (2001). *The elements of statistical learning*, Volume 1. Springer series in statistics New York.
- Guo, Y. (2013). Convex subspace representation learning from multi-view data. In *Twenty-Seventh AAAI Conference on Artificial Intelligence*.
- Hoerl, A. E. and R. W. Kennard (1970). Ridge regression: Biased estimation for nonorthogonal problems. *Technometrics* 12(1), 55–67.
- Kanehisa, M. (2000). *Post-genome informatics*. OUP Oxford.
- Li, C. and H. Li (2008). Network-constrained regularization and variable selection for analysis of genomic data. *Bioinformatics* 24(9), 1175–1182.
- Li, C. and H. Li (2010). Variable selection and regression analysis for graph-structured covariates with an application to genomics. *The annals of applied statistics* 4(3), 1498.

- Li, Q. and L. Li (2019). Integrative factor regression and its inference for multimodal data analysis. *arXiv preprint arXiv:1911.04056*.
- Lozupone, C. and R. Knight (2005). Unifrac: a new phylogenetic method for comparing microbial communities. *Applied and environmental microbiology* 71(12), 8228–8235.
- Neuhouser, M. L., Y. Schwarz, C. Wang, K. Breymeyer, G. Coronado, C.-Y. Wang, K. Noar, X. Song, and J. W. Lampe (2012). A low-glycemic load diet reduces serum c-reactive protein and modestly increases adiponectin in overweight and obese adults. *The Journal of nutrition* 142(2), 369–374.
- Ning, Y. and H. Liu (2017). A general theory of hypothesis tests and confidence regions for sparse high dimensional models. *The Annals of Statistics* 45(1), 158–195.
- Randolph, T. W., S. Zhao, W. Copeland, M. Hullar, and A. Shojaie (2018). Kernel-penalized regression for analysis of microbiome data. *The Annals of Applied Statistics* 12(1), 540–566.
- Reid, S., R. Tibshirani, and J. Friedman (2016). A study of error variance estimation in lasso regression. *Statistica Sinica*, 35–67.
- Rudelson, M., R. Vershynin, et al. (2013). Hanson-wright inequality and sub-gaussian concentration. *Electronic Communications in Probability* 18.
- Schaefer, C. F., K. Anthony, S. Krupa, J. Buchoff, M. Day, T. Hannay, and K. H. Buetow (2009). Pid: the pathway interaction database. *Nucleic acids research* 37(suppl\_1), D674–D679.
- Shao, J. and X. Deng (2012). Estimation in high-dimensional linear models with deterministic design matrices. *Ann. Statist.* 40(2), 812–831.
- Tibshirani, R. (1996). Regression shrinkage and selection via the lasso. *Journal of the Royal Statistical Society: Series B (Methodological)* 58(1), 267–288.

- van de Geer, S., P. Bühlmann, Y. Ritov, and R. Dezeure (2014). On asymptotically optimal confidence regions and tests for high-dimensional models. *The Annals of Statistics* 42(3), 1166–1202.
- van de Geer, S. A., P. Bühlmann, et al. (2009). On the conditions used to prove oracle results for the lasso. *Electronic Journal of Statistics* 3, 1360–1392.
- Wainwright, M. J. (2019). *High-dimensional statistics: A non-asymptotic viewpoint*, Volume 48. Cambridge University Press.
- Wang, H., F. Nie, and H. Huang (2013). Multi-view clustering and feature learning via structured sparsity. In *International conference on machine learning*, pp. 352–360.
- Yatsunenkov, T., F. E. Rey, M. J. Manary, I. Trehan, M. G. Dominguez-Bello, M. Contreras, M. Magris, G. Hidalgo, R. N. Baldassano, A. P. Anokhin, A. C. Heath, B. Warner, J. Reeder, J. Kuczynski, J. G. Caporaso, C. A. Lozupone, C. Lauber, J. C. Clemente, D. Knights, R. Knight, and J. I. Gordon (2012). Human gut microbiome viewed across age and geography. *Nature* 486(7402), 222–227.
- Yu, G. and J. Bien (2019). Estimating the error variance in a high-dimensional linear model. *Biometrika* 106(3), 533–546.
- Zeevi, D., T. Korem, A. Godneva, N. Bar, A. Kurilshikov, M. Lotan-Pompan, A. Weinberger, J. Fu, C. Wijmenga, A. Zhernakova, et al. (2019). Structural variation in the gut microbiome associates with host health. *Nature* 568(7750), 43–48.
- Zhang, C.-H., J. Huang, et al. (2008). The sparsity and bias of the lasso selection in high-dimensional linear regression. *The Annals of Statistics* 36(4), 1567–1594.
- Zhang, C. H. and S. S. Zhang (2014). Confidence intervals for low dimensional parameters in high dimensional linear models. *Journal of the Royal Statistical Society: Series B (Statistical Methodology)* 76, 217–242.

- Zhao, S. and A. Shojaie (2016). A significance test for graph-constrained estimation. *Biometrics* 72(2), 484–493.
- Zhu, Y. and J. Bradic (2018). Linear hypothesis testing in dense high-dimensional linear models. *Journal of the American Statistical Association* 113(524), 1583–1600.